Genetics: Early Online, published on September 14, 2017 as 10.1534/genetics.117.300290

Diversification of Transcriptional Regulation Determines Subfunctionalization of Paralogous Branched Chain Aminotransferases in the Yeast *Saccharomyces cerevisiae*

James González[1], Geovani López[2], Stefany Argueta[1], Ximena Escalera-Fanjul[1], Mohamed el Hafidi[3], Carlos Campero-Basaldua[1], Joseph Strauss[4], Lina Riego-Ruiz[5] and Alicia González[1]*

[1]Departamento de Bioquímica y Biología Estructural, Instituto de Fisiología Celular, Universidad Nacional Autónoma de México, Ciudad de México, México.

[2]Subdivisión de Medicina Familiar, División de Estudios de Posgrado, Facultad de Medicina, Universidad Nacional Autónoma de México, Ciudad de México, México

[3]Instituto Nacional de Cardiología Ignacio Chávez, Departamento de Biomedicina Cardiovascular, México D. F., México.

[4]Fungal Genetics and Genomics Unit, Department of Applied Genetics and Cell Biology, BOKU-University of Natural Resources and Life Sciences, Campus Tulln, Tulln, Austria.

[5]División de Biología Molecular, Instituto Potosino de Investigación Científica y Tecnológica, San Luis Potosí, México.

- Running title: Diversification through regulation
- Key words: functional diversification, expression regulation, aminotransferases, amino acid metabolism, paralogous genes.
- Corresponding author: Alicia González [1]Departamento de Bioquímica y Biología Estructural, Instituto de Fisiología Celular, Universidad Nacional Autónoma de México, Ciudad de México, México. 0052 55 56225631, amanjarr@ifc.unam.mx

Article Summary

Paralogous Bat1/Bat2 aminotransferases are involved in synthesis or catabolism of branched-chain amino acids valine, isoleucine and leucine (VIL). On glutamine, *BAT1* biosynthetic function is induced by Gcn4 and Leu3-α-IPM transcriptional activation, whereas *BAT2* is repressed by Ure2-inactivation of Gln3 and Leu3 prevention of starvation-induced Gcn4 derepression and *BAT2* activation. On VIL, *BAT1* is repressed by blocking Leu4/Leu9 α-IPM synthesis, and Put3 inhibition of a novel α-IPM biosynthetic pathway via leucine degradation, while VIL catabolism is induced by Gln3- and Put3-mediated *BAT2* transcriptional activation. Thus, Gcn4, Leu3, Gln3, Put3 favor either *BAT1* or *BAT2* expression, promoting VIL biosynthesis or catabolism.

Abstract

Saccharomyces cerevisiae harbors *BAT1* and *BAT2* paralogous genes encoding branched chain aminotransferases (BCATs), showing opposed expression profiles and physiological role. Accordingly, in primary nitrogen sources such as glutamine, *BAT1* expression is induced, supporting Bat1-dependent valine-isoleucine-leucine (VIL) biosynthesis, while *BAT2* expression is repressed. Conversely, in the presence of VIL as sole nitrogen source, *BAT1* expression is hindered while that of *BAT2* is activated resulting in Bat2-dependent VIL catabolism. Presented results confirm that *BAT1* expression is determined by transcriptional activation through the action of the Leu3-α–IPM active isoform, and uncovers the existence of a novel α-IPM biosynthetic pathway operating in a *put3*Δ mutant grown on VIL, through Bat2-Leu2-Leu1 consecutive action. The classic α-IPM biosynthetic route operates in glutamine through the action of the leucine sensitive α-isopropylmalate synthases (α–IPMS). Presented results also show that *BAT2* repression in glutamine can be alleviated in an *ure2*Δ mutant or through Gcn4-dependent transcriptional activation. Thus, when *S. cerevisiae* is grown on glutamine, VIL biosynthesis is predominant and is preferentially achieved through *BAT1*, while on VIL as sole nitrogen source, catabolism prevails and is mainly afforded by *BAT2*.

Introduction

Gene duplication is a key evolutionary mechanism resulting in the emergence of diversified genes, with new or specialized functions (Ohno 1970; Zhang 2003; Conant and Wolfe 2008). Phylogenomic studies have indicated that the contemporaneous occurrence of interspecies hybridization and genome duplication, have driven the acquisition of the genome organization, which is currently observed in *Saccharomyces cerevisiae* (*S. cerevisiae*) (Wolfe and Shields 1997; Marcet-Houben and Gabaldón 2015). After whole genome duplication, functional normal ploidy was recovered, as a result of the loss of 90% of duplicated genes (Mewes *et al*. 1997). In addition, selective retention and subfunctionalization of gene pairs derived from ancestral bifunctional genes have lead to the distribution of the ancestral function (s) between the paralogous copies (DeLuna *et al*. 2001; Quezada *et al*. 2008; López *et al*. 2015). Various modes of gene diversification have been described, which include modification of the oligomeric organization, kinetic properties, subcellular relocalization of the paralogous enzymes (DeLuna *et al*. 2001; Quezada *et al*. 2008; Colón *et al*. 2011; López *et al*. 2015), and diversification of the regulatory profile of paralogous genes (DeLuna *et al*. 2001; Avendaño *et al*. 2005). In *S. cerevisiae*, analysis of the expression patterns of duplicated genes has shown that transcriptional divergence occurs at a rapid rate in evolutionary time, and that differential or opposed expression amongst paralogous pairs could result from the acquisition of modified properties of both, the *trans*-acting factors (TFs) and the *cis*-acting elements, which constitute promoter binding sites to which TFs are recruited. Worth mentioning is the fact that it has also been proposed that modification of *cis* and *trans*-acting elements does not by itself account for expression diversification and that additional factors, such as mRNA

stability and local chromatin environment should also be considered (Makova and Li 2003; Gu *et al*. 2004; Zhang *et al*. 2004; Gu *et al*. 2005; Leach *et al*. 2007).

S. cerevisiae paralogous genes *BAT1* and *BAT2* encode Bat1 and Bat2 branched-chain aminotransferases (BCATs), which catalyze the first step of the catabolism and the last step of the biosynthesis of Branched Chain Amino Acids (BCAAs), namely-Valine, Isoleucine and Leucine (VIL) (Kispal *et al*. 1996; Eden *et al*. 2001) (Figure 1). *BAT1* and *BAT2* arose from the above mentioned hybridization and whole genome duplication event (WGD), which occurred about 100-150 million years ago (Marcet-Houben and Gabaldón 2015; Kellis *et al*. 2004). Previous work from our laboratory has shown that the ancestral-type yeasts *Kluyveromyces lactis* (*K. lactis*) and *Lachancea kluyveri* (*L. kluyveri*) which descend from the pre-WGD ancestor (Kellis *et al*. 2004), have a single *BAT* gene, respectively *KlBAT1* and *LkBAT1*, encoding bifunctional enzymes, involved in both VIL biosynthesis and catabolism (Colón *et al*. 2011; Montalvo-Arredondo *et al*. 2015). This dual function has been partitioned among the Bat1 and Bat2 paralogous proteins of *S. cerevisiae*. It has been further proposed that functional specialization occurred through Bat1 and Bat2 differential subcellular localization, and *BAT1* and *BAT2* expression divergence (Colón *et al*. 2011). Earlier studies from our group have indicated that *BAT1* shows a biosynthetic expression profile: repressed when VIL is provided in the medium, and induced in the absence of VIL, on either primary nitrogen sources such as ammonium or glutamine or on secondary nitrogen sources such as GABA (Colón *et al*. 2011). Furthermore, it has been shown that *BAT1* induced expression is primarily dependent on Leu3-α-IPM transcriptional activation (Sze *et al*. 1992), as opposed to *BAT2* regulation. Our group has also demonstrated that *BAT2* shows a catabolic expression pattern, which

136 resembles classic Nitrogen Catabolite Repression (NCR) profile (Blinder and Magasanik
137 1995; Coffman *et al*. 1995; Courchesne and Magasanik 1988; Minehart and Magasanik
138 1991), down-regulated in the presence of primary nitrogen sources such as glutamine, and
139 up-regulated in secondary nitrogen sources such as GABA or VIL (Colón *et al*. 2011).
140 Accordingly, in the presence of VIL as sole nitrogen source *BAT2* expression is induced,
141 confirming its catabolic expression profile as opposed to the biosynthetic expression pattern
142 displayed by *BAT1*.

143 Considering that *BAT1* and *BAT2* represent an interesting model to study the role of
144 expression divergence on functional diversification, we have analyzed the mechanisms
145 involved in *BAT1* and *BAT2* transcriptional regulation. Our results confirmed previous
146 observations (Boer *et al*. 2005) indicating that *BAT1* expression under biosynthetic
147 conditions is mainly achieved through Leu3-α-IPM. Nucleosome Scanning Assay (NuSA)
148 showed that Leu3 binding site is located in the Nucleosome Free Region (NFR) of *BAT1*
149 promoter, indicating Leu3 free accessibility to the promoter, on either glutamine or VIL.
150 The fact that on VIL as sole nitrogen source, *BAT1* expression is repressed (biosynthetic
151 expression profile), suggests that under this condition, lack of α-IPM could be hindering
152 Leu3-dependent transcriptional activation. Accordingly, our results show that a Put3-
153 dependent negative mechanism, which is elicited in a *put3*Δ mutant and suppressed in a
154 *put3*Δ *leu3*Δ double mutant, exerts an indirect negative action, hindering Leu3-α-IPM
155 positive role on *BAT1* transcription. Since in the presence of VIL, α-IPM biosynthesis is
156 inhibited (López *et al*. 2015), the existence of a VIL insensitive α-isopropylmalate (α-IPM)
157 biosynthetic pathway could support α-IPM production and formation of Leu3-α-IPM active
158 isoform. Presented results show that in a *put3*Δ mutant, the combined action of Bat2-Leu2-

159 Leu1, constitutes an α-IPM leucine insensitive biosynthetic pathway. In regard to *BAT2*
160 expression profile, it was found that on glutamine as sole nitrogen source, *BAT2* repression
161 is determined by the indirect negative effect of Ure2, as has been reported for other
162 catabolic genes (Blinder and Magasanik 1995; Coffman *et al*. 1995; Courchesne and
163 Magasanik 1988; Minehart and Magasanik 1991). In addition, presented results uncover the
164 existence of a negative Leu3 dependent role, which suppresses *BAT2* expression on
165 glutamine. In a *leu3*Δ mutant, amino acid deprivation is elicited, allowing *BAT2* induced
166 expression through Gcn4. Furthermore, NuSA analysis indicated that *BAT2* transition from
167 repressed (glutamine) to induced (VIL) expression is accompanied by chromatin
168 remodeling.

169 Our results underscore the fact that direct or indirect opposed regulatory action of
170 *trans*-acting factors, location of *cis*-acting elements in *BAT1* and *BAT2* promoters,
171 chromatin organization and the metabolic status of the cell, afford crucial pathways which
172 have influenced the functional role of the paralogous branched chain aminotransferases in
173 *S. cerevisiae.*
174

Materials and Methods

Growth conditions

Strains were grown on MM containing salts, trace elements, and vitamins according to the formula for yeast nitrogen base (Difco). Glucose (2% w/v) was used as carbon source, glutamine (Gln) (7 mM), γ-aminobutiric acid (GABA) (7mM), or valine (V) (150 mg/l) + leucine (L) (100 mg/l) + isoleucine (I) (30 mg/l) were used as nitrogen sources. Uracil (20 mg/l) and leucine (L) (100 mg/l) were added as auxotrophic requirements when needed. Cells were incubated at 30°C with shaking (250 rpm).

In silico promoter analysis

We examined a 600 bp intergenic region upstream of the start codon of the branched chain amino acid transaminase genes of *S. cerevisiae* genome. The 1500 bp sequences upstream of the predicted start codon were subject to *in silico* promoter analysis (Figures S1 and S2). All genomic sequences analyzed in this study were obtained from YGOB database (Byrne and Wolfe, 2005). Sequences were subject to motif scanning using the "Matrix Scan" program, a member of the "RSA tools" package (Van Helden, 2003; Turatsinze *et al*., 2008; Thomas-Chollier *et al*., 2008 ; Thomas-Chollier *et al*., 2011). The yeast transcription factor matrix motifs used for this analysis were downloaded from the "YeTFaSCo" database (de Boer and Hughes, 2012).

Strains

S. cerevisiae strains used in this work are described in Table 1.

Table 1. Yeast strains used in this study.

Strain	Genotype	Source
CLA11-700	*S. cerevisiae MATα ura3 leu2::LEU2*	(DeLuna *et al*. 2001)
BY4741 *PUT3*-TAP	*S. cerevisiae ura3 leu2 his3 met5 PUT3-TAP*	(TAP collection)
CLA11-706	*MATα ENO2pr-LEU4 ENO2-prLEU9 leu2::LEU2*	(López *et al*.2015)
CLA11-708 *gcn4*Δ	*MATα gcn4::kanMX4 ura3 leu2::LEU2*	This study
C1LA1-709 *leu3*Δ	*MATα leu3::kanMX4 ura3 leu2::LEU2*	This study
CLA11-710 *gln3*Δ	*MATα gln3::kanMX4 ura3 leu2::LEU2*	This study
CLA11-711 *put3*Δ	*MATα put3::kanMX4 ura3 leu2::LEU2*	This study
CLA11-712 *ure2*Δ	*MATα ure2::kanMX4 ura3 leu2::LEU2*	This study
CLA11-713 *nrg1*Δ	*MATα nrg1::kanMX4 ura3 leu2::LEU2*	This study
CLA11-714 *gat1*Δ	*MATα gat1::kanMX4 ura3 leu2::LEU2*	This study
CLA11-715 *hap2*Δ	*MATα hap2::kanMX4 ura3 leu2::LEU2*	This study
CLA11-716 *mot3*Δ	*MATα mot3::kanMX4 ura3 leu2::LEU2*	This study
CLA11-717 *leu3*Δ	*MATα leu3::natMX4 ura3 leu2::LEU2*	This study
CLA11-719 *put3*Δ*leu1*Δ	*MATα put3::kanMX4 leu1::URA3 leu2::LEU2*	This study
CLA11-720 *gcn4*Δ*leu3*Δ	*MATα gcn4::kanMX4 leu3::natMX4 ure3 leu2::LEU2*	This study
CLA11-721 *put3*Δ*leu3*Δ	*MATα put3::kanMX4 leu3::natMX4 ure3 leu2::LEU2*	This study
CLA11-722 *ure2*Δ*gln3*Δ	*MATα ure2::kanMX4 gln3::natMX4 ura3 leu2*	This study
CLA11-723 *GCN4-myc*^{13}	*MATα GCN4-myc*^{13}*::kanMX4 ura3 leu2::LEU2*	This study
CLA11-724 *GLN3-myc*^{13}	*MATα GLN3-myc*^{13}*::kanMX4 ura3 leu2::LEU2*	This study
CLA11-725 *LEU3-myc*^{13}	*MATα LEU3-myc*^{13}*::kanMX4 ura3 leu2::LEU2*	This study
CLA11-726 *gata*$_{boxes}$	*MATα* P_{BAT1} *GATAAT::GcaAAT, GATAAA::GcaAAA, GATAAT:: GcaAAT, GATAAG::GcaAAG ura3 leu2::LEU2*	This study
CLA11-727 *leu3*$_{box}$	*MATα* P_{BAT1} *GCCGGTACCGGC::aaaGGTACCaaa ura3 leu2::LEU2*	This study
CLA11-728 *put3*$_{box}$	*MATα* P_{BAT1} *CGCTGGATAAGTACCG::aaaTGGATAAGTAaaa ura3 leu2::LEU2*	This study
CLA11-729 *gata*$_{box}$	*MATα* P_{BAT2} *GTTATC::GTTtgC ura3 leu2::LEU2*	This study
CLA11-730 *leu3*$_{box}$	*MATα* P_{BAT2} *CCGCTTTCGG::CCGCTTTaaa ura3 leu2::LEU2*	This study
CLA11-731 *put3*$_{box}$	*MATα* P_{BAT2} *CGGCGTTCTTTTTCGG::aaaCGTTCTTTTTCGG ura3 leu2::LEU2*	This study
CLA11-732	*MATα* P_{ENO2}*LEU4* P_{ENO2}*LEU9 leu1::URA3 leu2::LEU2*	This study
CLA11-733 *leu4*Δ*leu9*Δ	*MATα leu4::URA3 leu9::kanMX4 leu2::LEU2*	(López *et al*. 2015)
CLA11-734 *GCN4-myc*^{13}*leu3*Δ	*MATα GCN4-myc*^{13}*::kanMX4 ura3 leu2::LEU2*	This study
CLA11-735 *LEU3-myc*^{13}*leu3*$_{box}$	*MATα* P_{BAT2} *CCGCTTTCGG::CCGCTTTaaa LEU3-myc*^{13}*::kanMX4 ura3 leu2::LEU2*	This study
CLA11-736 *leu4*Δ*leu9*Δ*leu1*Δ	*MATα leu4::kanMX4 leu9::natMX4 leu1::URA3 leu2::LEU2*	This study
CLA11-737 *put3*Δ*bat2*Δ	*MATα put3::kanMX4 bat2::natMX4 ura3 leu2::LEU2*	This study

All *S. cerevisiae* strains are isogenic derivatives of the previously described CLA11-700 (*MATα leu2::LEU2 ura3*) (DeLuna *et al*. 2001). The isogenic *gcn4*Δ (CLA11-708), *leu3*Δ

(CLA11-709), *gln3*Δ (CLA11-710), *put3*Δ (CLA11-711), *ure2*Δ (CLA11-712), *nrg1*Δ (CLA11-713), *gat1*Δ (CLA11-714), *hap2*Δ (CLA11-715) and *mot3*Δ (CLA11-716) were obtained from strain CLA11-700 by gene replacement. A PCR-generated *kanMX4* module was prepared from plasmid pFA6a (Table S1) following a previously described method (Longtine *et al*. 1998) using J1 to J18 deoxyoligonucleotides (Table S2). Double mutants were constructed as follows. The *kanMX4* module from CLA11-709 *leu3*::*kanMX4* was replaced by the *natMX4* cassette, which confers resistance to the antibiotic nourseothricin (Goldstein and McCusker 1999). The *natMX4* cassette used for transformation was obtained by digesting plasmid p4339 (Table S1) with *Eco* RI. The *leu3*::*natMX4* strain (CLA11-717) was transformed following a previously described method (Ito *et al.* 1983). Double *put3*Δ *leu1*Δ (CLA11-719) and *put3*Δ *bat2*Δ (CLA11-737) were prepared by transforming the *put3*Δ (CLA11-711) by inserting a PCR module containing the *URA3* gene amplified from plasmid pKT175 (Sheff and Thorn, 2004) in *LEU1*, or the *natMX4* module from plasmid p4339 (Table S1) to delete *BAT2* using J19-J20 or J20A-J20B deoxyoligonucleotides respectively (Table S2). The double *gcn4*Δ *leu3*Δ (CLA11-720), *put3*Δ *leu3*Δ (CLA11-721) mutants were prepared by transforming the *leu3*Δ (CLA11-717) with *kanMX4* modules respectively replacing *GCN4* or *PUT3* using the deoxyoligonucleotides described in Table S2 (J1-J2 or J7-J8, respectively). Double mutant *gln3*Δ *ure2*Δ (CLA11-722) was constructed replacing *GLN3* and *URE2* by *natMX4* and *kanMX4* modules as described above. Transformants were selected for either G418 resistance (200 mg/l; Life Technologies, Inc.), or nourseothricin resistance (100 mg/l; Werner Bio Agents), on yeast extract-peptone-dextrose (YPD)-rich medium. Single and double mutants were PCR verified. The triple *leu4*Δ *leu9*Δ *leu1*Δ (Strain CLA11-736) mutant was obtained from strain CLA11-700 by gene replacement. Three PCR modules

(*kanMX4*, *natMX4*, and *URA3*) were prepared from plasmids; pFA6a, p4339 and pKT175 (Table S1) following a previously described method (Longtine *et al*. 1998) using J20C-J20D, J20E-J20F and J19-J20 deoxyoligonucleotides (Table S2). *LEU4*, *LEU9* and *LEU1* *loci* were replaced by the *kanMX4*, *natMX4* and *URA3* modules respectively. Transformants were simultaneously selected for both G418 resistance and nourseothricin resistance on yeast extract-peptone-dextrose (YPD)-rich medium as described above. Transformants resistant to nourseothricin and G418 were selected on plates with MM plus glucose without uracil. Triple mutant was PCR verified. The strain CLA11-732 (MATα P_{ENO2}*LEU4* P_{ENO2}*LEU9 leu1::URA3 leu2::LEU2*) was prepared from the isogenic strain CLA11-706 (MATα *ENO2pr-LEU4 ENO2pr-LEU9 leu2::LEU2*) (López *et al*. 2015), by inserting a PCR module containing the *URA3* gene amplified from plasmid pKT175 (Sheff and Thorn, 2004) in *LEU1* using J19-J20 deoxyoligonucleotides (Table S2). *PUT3*-TAP BY4741 *ura3 leu2 his3 met5* was obtained from the TAP-tagged *Saccharomyces* strain collection.

Construction of myc-tagged strains

GCN4-myc^{13} (CLA11-723), *GLN3-myc*^{13} (CLA11-724) and *LEU3-myc*^{13} (CLA11-725) strains were tagged with the 13-myc-*kanMX4* module obtained from plasmid pFA6a-*myc*^{13}-kanMX6 (Goldstein and McCusker, 1999) (Table S3) using J21 to J26 deoxyoligonucleotides (Table S3). *GCN4-myc*^{13}*leu3*Δ (CLA11-734) strain was prepared from the *GCN4-myc*^{13} (CLA11-723) isogenic strain, *LEU3* locus was replaced with the *leu3*::*natMX4* module obtained from *leu3*::*natMX4* (CLA11-717) strain by homologous recombination, using J26-A and J26-B deoxyoligonucleotides (Table S3). *LEU3-myc*^{13}

leu3$_{box}$ (CLA11-735) strain was prepared from CLA11-730 *leu3*$_{box}$ (MATα P_{BAT2} CCGCTTTCGG::CCGCTTTaaa *ura3 leu2::LEU2*), *LEU3* was tagged with the 13-myc-*kanMX4* module obtained from plasmid pFA6a-*myc*^{13}-kanMX6 using J25-J26 deoxyoligonucleotides (Table S3). Transformants were selected for G418 resistance (200 mg/l; Life Technologies, Inc.), or nourseothricin resistance (100 mg/l; Werner Bio Agents), on yeast extract-peptone-dextrose (YPD)-rich medium. Strains were PCR verified.

Northern blot analysis

Northern blot analysis was performed as described earlier (Valenzuela *et al*. 1998). Total yeast RNA was extracted following the method of Struhl and Davis 1981. Cultures were grown to an OD_{600} ~0.5 in MM with glutamine (Gln) or valine+isoleucine+leucine (VIL) as sole nitrogen sources, and 2% glucose as carbon source, 50 ml aliquots were used to obtain total RNA. PCR specific products for *BAT1*, *BAT2*, *ACT1*, *SCR1*, *DAL5*, *HIS4*, *LEU1* and *LEU2* were generated from genomic DNA using J27 to J50 deoxyoligonucleotides (Table S4), and radioactively labeled by α-32P dCTP with Random Primer Labeling Kit (Agilent Cat# 300385). These were respectively used as hybridization probes for the mRNA of *BAT1*, *BAT2*, *ACT1*, *SCR1*, *DAL5*, *HIS4*, *LEU1* and *LEU2*. Blots were scanned with the Image Quant 5.2 (Molecular Dynamics) program. Representative results of three experiments are presented.

278 ***Nucleosome Scanning Assay***

279

280 Nucleosome scanning experiments were performed adapting a previously described method
281 (Biddick *et al*. 2008; Infante *et al*. 2012). Wild-type *S. cerevisiae* strain was grown in 50 ml
282 MM 2% glucose with 7 mM glutamine (Gln) or Valine (V) (150 mg/l) + Isoleucine (I) (30
283 mg/l) + Leucine (L) (100 mg/l) to a ~0.5 $OD_{600.}$ One percent final formaldehyde
284 concentration was added for 20 min at 37 ℃ after which 125mM glycine was supplied for
285 5 min at 37 ℃. Formaldehyde-treated cells were harvested by centrifugation, washed with
286 Tris-buffered saline, and then incubated in Buffer Z2 (1M Sorbitol, 50 mM Tris-Cl at pH
287 7.4, 10 mM β-mercaptoethanol) containing 2.5 mg of zymolase 20T for 20 min at 30 ℃ on
288 a shaker. Spheroplasts were pelleted by centrifugation at 3000 x g, and resuspended in 1.5
289 ml of NPS buffer (0.5 mM Spermidine, 0.075% NP-40, 50 mM NaCl, 10 mM Tris pH 7.4,
290 5 mM $MgCl_2$, 1 mM $CaCl_2$, 1 mM β-mercaptoethanol). Samples were divided in three 500
291 µl aliquots which were then digested with 22.5 U of MNase (Nuclease S7 from Roche) at
292 50 min at 37 ℃. Digestions were interrupted with 12 µl of stop buffer (50 mM EDTA and
293 1% SDS) and treated with 100 µg of proteinase K at 65 ℃ overnight. DNA was extracted
294 twice with phenol/chloroform and precipitated with 20 µl of 5 M NaCl and an equal
295 volume of isopropanol for 30 min at -20 ℃. Precipitates were then resuspended in 40 µl of
296 TE buffer and incubated with 20 µg RNase A for 1 h at 37 ℃. DNA digestions were
297 performed as previously reported (Infante *et al*. 2012). Monosomal bands were cut and
298 purified by Wizard SV Gel Clean-Up System Kit (Promega, REF A9282). DNA samples
299 were diluted 1:30 and used for quantitative polymerase chain reactions (qPCR) to
300 independently determine relative MNase protection of *BAT1* (YHR208W) and *BAT2*
301 (YJR148W) templates. qPCR analysis was performed using a Corbett Life Science Rotor

Gene 6000 machine. SYBR Green was used as detection dye (2× KAPA SYBR FASTq Bioline and Platinum SYBR Green from Invitrogen). Quantitative PCR was carried out as follows: 94° for 5 min (1 cycle), 94° for 15 sec, 58° for 20 sec, and 72° for 20 sec (35 cycles). *BAT1* and *BAT2* relative protection was respectively calculated as a ratio considering amplification of a region of *VCX1,* with the following deoxyoligonucletide pairs: Fw 5'- TGC GTG TGC ATC CCT ACT GA -3' and Rv 5'- AAG TGG TCT TCC TTG CCA TGA -3'. PCR deoxyoligonucleotides are described in S5 and S6 Tables, which amplify from around -600 pb to +250 bp of *BAT1* or *BAT2* loci whose coordinates are given relative to the ATG +1. All presented nucleosome scanning assays represent the mean values and standard errors of at least three independent biological replicates.

Metabolite extraction and analysis

Cell extracts were prepared from exponentially growing cultures (OD_{600} 0.3 and 0.6). Samples used for intracellular amino acid determination were treated as previously described (Quezada *et al*. 2008).

Quantitative Chromatin Immunoprecipitation

Formaldehyde cross-linking and immunoprecipitations were carried out adapting a previously described procedure (Hernández *et al.* 2011). Yeast cells (200 ml of OD_{600} 0.5) were cross-linked with 1% formaldehyde for 20 min at room temperature. Afterwards, 125 mM glycine was added and incubated for 5 min. Cells were then harvested and washed with PBS buffer. Pelleted cells were suspended in lysis buffer (140 mM NaCl, 1 mM

EDTA, 50 mM HEPES/KOH, 1 % Triton X-100, 0.1 % sodium deoxycholate) with a protease inhibitor cocktail (Complete Mini, Roche). Cells were lysed with glass beads and collected by centrifugation. Extracts were sonicated with a Diagenode Bioruptor to produce chromatin fragments average size of 300 bp. Immunoprecipitation reactions were carried out with 1 mg anti-c-Myc antibody (9E 11, Santa Cruz Biotechnology) and protein A beads for 3 h, washed, suspended in TE buffer / 1 % SDS and incubated overnight at 65°C in order to reverse the formaldehyde cross-linking. Immunoprecipitates were then incubated with proteinase K (Roche) followed by phenol/chloroform/isoamyl alcohol extraction, precipitated and suspended in 30 µl TE buffer. Dilutions of input DNA (1:100) and immunoprecipitated DNA (1:2) were analyzed by qPCR. Real-time PCR-based DNA amplification was performed using specific primers that were initially screened for dimer absence or cross-hybridization. Only primer pairs with similar amplification efficiencies were used (Table S7). Quantitative chromatin immunoprecipitation (qChIP) analysis was performed using a Corbett Life Science Rotor Gene 6000 machine. The fold difference between immunoprecipitated material (IP) and total input sample for each qPCR amplified region was calculated following the formula IP/Input = ($2^{InputCt - IPCt}$) (Litt *et al.* 2001). Results presented represent the mean values and standard errors of at least three independent cross-linked samples with each sample being immunoprecipitated twice with the antibody.

Construction of site-specific DNA mutations

Mutants altered in *cis*-acting elements were constructed by transforming wild-type strain CLA11-700 with a 3.2 kb fragment obtained by PCR amplification of the pCORE plasmid

harbouring the *kanMX4* and *URA3 CORE* modules (Storci and Resnick, 2003). Transformations were carried out following the previously described protocol (Ito *et al*. 1983). Colonies were isolated on YPD-G418 (200 mg/l). Correct insertion was verified by PCR amplification. Transformants were retransformed with IROs (Integrative Recombinant Oligonucleotides) harbouring mutagenized modules (Table S8, Figure S3). Generated strains were CLA11-726 (*GATA* boxes at positions -424, -415, -374 and -324 in *BAT1* promoter, from G**AT**AAT, G**AT**AAA, G**AT**AAT and G**AT**AAG to G**ca**AAT, G**ca**AAA, G**ca**TAAT and G**ca**AAG), CLA11-727 (*LEU3* binding site at positions -150 and -141 *BAT1* promoter, from **GCC**GGTACC**GGC** to **aaa**GGTACC**aaa**), CLA11-728 (*PUT3* binding site at positions -163 and -150 in *BAT1* promoter, from **CGC**TGGATAAGTA**CCG** to **aaa**TGGATAAGTA**aaa**), CLA11-729 (*GATA* box at position -282 in *BAT2* promoter, from GTT**AT**C to GTT**tg**C), CLA11-730 (*LEU3* binding site at position -327 in *BAT2* promoter, from **CCG**CTTT**CGG** to **CCG**CTTT**aaa**), and CLA11-731 (*PUT3* binding site at position -347 in *BAT2* promoter, from **CGG**CGTTCTTTTTCGG to **aaa**CGTTCTTTTTCGG). After transformation, FOA-resistant colonies were analyzed by PCR. Correct insertion was confirmed by sequencing with an Applied Biosystems 3100 Genetic Analyzer.

Data availability

The 32 strains listed in Table 1 and plasmids described in Table S1 are available upon request. Sequences performed to confirm *cis* elements mutants are described in Figure S3. Date concerning sequences analysis of TF binding sites and mutants phenotypes are presented in Figures S1, S2, S4, S5 and S6.

Results

Identification of the presumed cis-acting elements located on the BAT1 and BAT2 promoters and assessment of their accessibility by nucleosome scanning assay

To identify the presumed *cis*-acting factors that could influence *BAT1* and *BAT2* expression, DNA sequence of both promoter regions was analyzed with the pertinent bioinformatic tools (Materials and Methods). Occupancy of the *cis*-acting sequences were assessed by analyzing the chromatin organization profile determined by Nucleosome Scanning Assay (NuSA). As a positive control, gene expression was monitored by Northern analysis in samples obtained from the same cultures from which chromatin organization assays of *BAT1* and *BAT2* promoters were performed (OD_{600} 0.5), as described in Materials and Methods. As expected, expression analysis confirmed the previously reported *BAT1* biosynthetic profile (VIL repressed), and *BAT2* catabolic profile (VIL induced), since, expression is only observed in the presence of VIL (Colón *et al*. 2011) (Figure 2A).

NuSA assays, were carried out to determine nucleosome positioning and occupancy of presumed *cis*-acting elements across the *BAT1* and *BAT2* promoters in wild-type cells grown on glutamine or VIL as sole nitrogen sources. Quantitative PCR (qPCR) was respectively carried out with 30 or 29 primer pairs for *BAT1* or *BAT2* (Tables S5 and S6), to independently amplify overlapping regions of both promoters (Figures 2B and C). Peaks of relative protection indicated that in either glutamine or VIL, four nucleosomes were similarly positioned around the *BAT1* transcriptional starting point (-2, -1, +1 and +2) (Figure 2B). Nucleosome -1 and +1 constitute the border of the 150-bp MNase-sensitive

Nucleosome Free Region (NFR), which spans from around -200 to -100 with respect to the *BAT1* +1 ATG (Figure 2B), indicating that *BAT1* differential expression on glutamine or VIL does not require chromatin remodeling. The presumed *cis*-acting elements present in the *BAT1* and *BAT2* promoters, were identified through a comparative *in silico* analysis of their location (Figures 3A and B). For *BAT1* the *HAP2, MOT3, GCN4* and *LEU3* presumed binding sites were located within the NFR (Figures 2B and 3A). *BAT2* promoter NuSA analysis revealed that in glutamine, at least four nucleosomes designated -2, -1, +1 and +2, were firmly positioned (Figure 2C), indicating occupation of the $TATA_{BOX}$ in accordance with glutamine-repressed expression pattern (Figure 2A). The NuSA profile observed on VIL for the *BAT2* promoter showed that the region from -150 to -50, harboring the $TATA_{BOX}$, was nucleosome free, suggesting higher expression as compared to that observed on glutamine. It was also found that *NRG, HAP2, LEU3, PUT3* sites would be nucleosome protected in either glutamine or VIL, whereas the *GLN3-GAT1 cis*-acting elements would be exposed under both conditions and *GCN4* only uncovered on VIL (Figures 2C and 3B). It can thus be proposed that *BAT2* differential regulation on glutamine or VIL could be impacted by chromatin remodeling.

Gln3, Gcn4, Leu3 and Put3 trans-acting factors, determine BAT1 and/or BAT2 expression profile

To analyze whether the *trans*-acting elements that should bind the above described *cis*-acting factors had a role in *BAT1* and *BAT2* expression, deletion mutants were constructed in the corresponding coding genes: *GLN3-GAT1* (Blinder and Magasanik 1995), *NRG1*

(Zhou and Winston, 2001), *LEU3* (Kohlaw 2003; Friden and Schimel 1988), *PUT3* (Siddiqui and Brandriss 1989), *MOT3* (Martinez-Montanes *et al*. 2013), *GCN4* (Hinnebusch and Fink 1983; Hinnebusch 1984) and *HAP2* (Guarente *et al*. 1984). As shown in Figure S4, *nrg1*Δ , *gat1*Δ , *hap2*Δ and *mot3*Δ mutant strains showed *BAT1* and *BAT2* wild-type expression profiles, indicating that under the conditions tested, the encoded regulators played no role on *BAT1* or *BAT2* transcriptional regulation. Northern blot analysis was carried out on samples obtained from cultures in which Gln GABA or VIL were used as sole nitrogen sources, confirming previously observed effect of both the quality of the nitrogen source and the peculiar effect of VIL on *BAT1* and *BAT2* expression (Colon *et al*., 2011). As opposed to that found for *NRG1, GAT1, HAP2* and *MOT3* mutants, *gcn4*Δ, *leu3*Δ, *gln3*Δ and *put3*Δ displayed a distinct phenotype when Northern blot analysis was carried out on total RNA samples (Figures 4A and 5A).

Role of Gcn4 and Gln3 trans-acting factors on BAT1 and/or BAT2 expression profile

When total RNA was prepared from glutamine grown cells (biosynthetic conditions), it was found that Gcn4 and Gln3 displayed a positive effect on *BAT1* transcriptional activation, showing no adverse effects on that of *BAT2* (Figure 4A). On VIL (catabolic conditions) grown yeasts, Gln3 played a positive role on *BAT1* expression but showed no adverse effects on that of *BAT2*, while Gcn4 showed no effect on either *BAT1* or *BAT2* expression on this condition (Figure 4A).

To analyze whether Gln3 and Gcn4 were acting by direct binding on *BAT1* and *BAT2* promoters, quantitative chromatin immunoprecipitation (qChIP) experiments were

carried out as described in Materials and Methods. To this end, Gcn4-*myc*^{13}, Gln3-*myc*^{13} derivatives were constructed (Materials and Methods), and their capacity to sustain wild type transcriptional regulation was assessed (Figure S5). Amplification of three different regions of *BAT1* (Figure 4B, R1-R3) or *BAT2* (Figure 4B, R1'-R3') promoters was analyzed by qChIP analysis. Gcn4-*myc*^{13} readily bound *BAT1* promoter, but not *BAT2* promoter (Figure 4C), in agreement with *gcn4*Δ mutant expression analysis, which showed that Gcn4 did not regulates *BAT2* expression (Figure 4A). It could also be considered that Gcn4 has a weak binding site on the *BAT2* promoter since as will be shown further on, increased Gcn4 concentration evoked in a *leu3*Δ mutant, allows Gcn4-*myc*^{13} binding to *BAT2* promoter in glutamine (Figure 7B). As positive control, binding of Gcn4-*myc*^{13} to *HIS4* was monitored. It was observed that although Gcn4-*myc*^{13} clearly bound *HIS4* promoter on samples prepared from glutamine and GABA grown cultures, binding on VIL obtained samples was scarce as compared to that found on either glutamine or GABA. It has been shown that Gcn4 concentration is tightly regulated through the combined action of a complex translational control mechanism, which induces Gcn4 synthesis in starved cells, and a phosphorylation and ubiquitylation pathway that mediates its rapid degradation by the proteasome (Rawal *et al*. 2014; Hinnebusch 2005). However, Gcn4 abundance has not been determined in cultures grown on VIL as sole nitrogen source, and there is no evidence suggesting Gcn4 preferential degradation under this condition. Thus, the herein reported observation could be attributed to the fact that in the presence of leucine, TOR1C-dependent m*GCN4* translatiom is impaired (Kingsbury *et al*, 2015, Valenzuela *et al*, 2001). However, our results indicate that Gcn4-*myc*^{13} is bound to *BAT1* and *HIS4* promoters on glutamine and GABA, confirming *BAT1* is a direct Gcn4 target.

As expected, Gln3-*myc*^{13} bound *BAT2* promoter in the presence of VIL or GABA secondary non-repressive nitrogen sources, but not on glutamine, which is a primary repressive nitrogen source (Figure 4D) (Courchesne and Magasanik 1988), in agreement with *BAT2* observed expression in a *gln3*Δ mutant (Figure 4A). Gln3 did not bind *BAT1* promoter under any of the conditions tested, although it showed a positive regulatory input on *BAT1* expression on glutamine and VIL (Figures 4A and D). As this effect is rather mild and Gln3 cannot be detected at *BAT1* promoter, through qChIP analysis, the observed deregulation is most likely to be afforded by an indirect effect. However, to further analyze whether Gln3 acted through its direct action on the promoters, we used *delitto perfetto* strategy to complement our results with *cis*-acting site-specific mutations on Gln3 consensus and/or conserved elements in *BAT1* and *BAT2* promoters. A mutation of the Gln3 presumed consensus-binding site (GATAAG) (Byasani *et al*. 1991) located at the *BAT2* promoter (*GLN3-GAT1*) resulted in decreased *BAT2* expression (Figure 4F). For *BAT1*, a simultaneous *cis*-mutation in each one of a cluster of four presumed *GLN3-GAT1* binding sites, did not affect expression (Figure 4E), confirming the observation that although *BAT1* expression on glutamine and VIL is partially activated through Gln3 (Figure 4A), the mechanism does not involve direct Gln3-promoter interaction and consequently, positive Gln3-dependent *BAT1* effect is indirect, while *BAT2* positive regulation through Gln3 is direct.

Put3 and Leu3 trans-acting factors, play a crucial role on BAT1 and BAT2 regulatory subfunctionalization determining opposed BAT1/BAT2 expression profile

To analyze Put3 and Leu3 role on *BAT1* and *BAT2* expression, total RNA was prepared from glutamine grown cells (biosynthetic conditions). It was found that as was previously observed (Boer *et al*. 2005), *BAT1* expression activation was achieved through Leu3 (Figure 5A). However, a previously unidentified negative role for Leu3 on *BAT2* expression was detected (Figure 5A), indicating that Leu3 played a role in glutamine-dependent *BAT2* repressed expression and consequently, Leu3 had opposing effects on *BAT1* and *BAT2* expression. Under this condition, Put3 did not play a role on either *BAT1* or *BAT2* expression profile (Figure 5A).

Northern analysis carried out on total RNA prepared from cells grown on VIL as sole nitrogen source, showed that *BAT1* expression was repressed. However, in a *put3*Δ mutant, expression was four-fold de-repressed as compared to that observed in a wild type *PUT3* strain indicating that this modulator played a negative role on *BAT1* transcriptional activation in media supplemented with VIL as sole nitrogen source (Figure 5A). Contrastingly, *BAT2* expression was Put3-activated (Figure 5A), indicating Put3 exerted opposed effects on *BAT1* and *BAT2* transcriptional activation on VIL grown yeast. Under this condition, Leu3 only played a positive role on *BAT1* expression, and no role on that of *BAT2*.

To analyze whether Leu3 was acting by direct binding on *BAT1* and *BAT2* promoters, quantitative chromatin immunoprecipitation (qChIP) experiments were carried out as described in Materials and Methods. To this end, Leu3-*myc*^{13} derivatives were

512 constructed (Materials and Methods), and the Put3-TAP mutant strain was obtained from
513 the *S. cerevisiae* collection (Table 1). The capacity to sustain wild type transcriptional
514 regulation by the *myc*^{13} or TAP tagged derivatives was confirmed for either Leu3-*myc*^{13} or
515 Put3-TAP (Figure S5). As presented for Gln3 and Gcn4 binding assays, three different
516 regions of the *BAT1* (Figure 5B, R1-R3) or *BAT2* (Figure 5B, R1'-R3') promoters were
517 selected to analyze Put3 and Leu3 binding through qChIP analysis. Put3-TAP was found to
518 bind *BAT2* (Figure 5C), indicating that observed *BAT2* transcriptional activation was
519 dependent on the direct action of Put3 on *BAT2* promoter. However, Put3 did not bind
520 *BAT1* promoter (Figure 5C), indicating that the negative role exerted by this *trans*-acting
521 factor was indirect. As positive control, Put3 binding to *PUT1* promoter was monitored
522 (Siddiqui and Brandriss 1989). Binding to *GRS1* promoter was used as negative control. On
523 the other hand, Leu3 was bound to both, *BAT1* and *BAT2* promoters in either nitrogen
524 repressive or non-repressing conditions (Figure 5D). As positive control, Leu3 binding to
525 *ILV5* (Friden and Schimmel 1988) was monitored and, *GRS1* was used as negative control.
526 To further analyze whether *trans*-acting factors acted through direct action on the
527 promoters, we used *delitto perfetto* strategy to obtain mutants affected in *cis*-acting specific
528 consensus and/or conserved sequences, in *BAT1* and *BAT2* promoters. Accordingly, the
529 mutation of the *LEU3 cis*-acting element present in the *BAT1* promoter displayed identical
530 phenotype to that of the *leu3*Δ mutant, decreasing *BAT1* expression on glutamine and VIL
531 (Figures 5A and E). Conversely, for *BAT2*, the mutation on the *LEU3 cis*-acting element
532 did not result in de-repressed expression on glutamine as that found in the *leu3*Δ mutant,
533 suggesting an indirect effect (Figures 5A and F). Mutation of the *PUT3* presumed *cis*-acting
534 element present in *BAT1*, did not result in de-repression on VIL, indicating an indirect

effect (Figures 5A and E), in agreement with the fact that Put3 did not bind *BAT1* promoter. While, a similar *cis*-acting mutation for *BAT2* promoter resulted in decreased transcriptional activation generating a phenotype equivalent to that found in a *put3*Δ mutant (Figures 5A and F), in agreement with the fact that Put3 bound *BAT2* promoter. It can be thus concluded that negative regulation of *BAT1* and *BAT2* respectively afforded through the action of Put3 or Leu3 is indirect, while *BAT1* and *BAT2* positive regulation respectively determined by Leu3 and Put3 is direct.

Under biosynthetic conditions (glutamine) Leu3 activates <u>BAT1</u> expression while that of <u>BAT2</u> is hindered through the negative and indirect action of Leu3 and Ure2 transcriptional regulation

Above results pose an interesting paradox in regard to Leu3 role on transcriptional regulation, because we show that in the presence of glutamine as nitrogen source Leu3 can either activate or repress gene expression (Figure 5A). These results apparently contradict the proposed mode of action for Leu3 as transcriptional regulator (Sze *et al*. 1992). The suggested model considers that in a given physiological condition, the intracellular α-IPM concentration should either allow the constitution of the Leu3-dimer that would act as negative regulator, preventing induction, or the Leu3-α-IPM dimer activator complex, which would determine induction of target genes. However, our results show that on glutamine as sole nitrogen source, Leu3 is able to support opposite expression responses: *BAT1* induction and *BAT2* repression (Figure 5A). To further analyze this matter, we constructed a double mutant in which the two genes (*LEU4* and *LEU9*) encoding α-

isopropylmalate synthase (α-IPMS) were expressed from the *ENO2* promoter resulting in α-IPM overproduction (López *et al*. 2015). Furthermore, to avoid α-IPM catabolism to β-isopropylmalate (β-IPM), *LEU1* gene, which encodes for the sole enzyme performing this function in *S. cerevisiae* was deleted in the P_{ENO2}*LEU4* P_{ENO2}*LEU9* mutant. The generated strain P_{ENO2}*LEU4* P_{ENO2}*LEU9 leu1*Δ should feature increased α-IPM biosynthesis and null catabolism. A second mutant was constructed harboring *leu4*Δ and *leu9*Δ deletions thus constituting a leucine auxotroph unable to synthesize α-IPM (Figure 6A), and the triple mutant *leu4*Δ *leu9*Δ *leu1*Δ, which would not be able to synthesize α-IPM, neither through the leucine sensitive pathway nor through the Bat2-Leu2-Le41 leucine resistant pathway. *BAT1* and *BAT2* expression was analyzed in these engineered strains (Figure 6B). *BAT1* expression was increased in the P_{ENO2}*LEU4* P_{ENO2}*LEU9 leu1*Δ triple mutant as compared to that found in the wild type strain, when grown on glutamine. Most important was the observation, that in this triple mutant *BAT1* was over-expressed even in the presence of VIL (Figure 6B), circumventing α-IPMS leucine sensitivity. As expected for a gene whose transcriptional activation is Leu3-α-IPM-dependent, increased α-IPM biosynthesis enhanced its transcriptional activation overcoming VIL mediated repression due to inhibition of α-IPM biosynthesis and the consequent lack of Leu3-α-IPM. The fact that in a *leu4*Δ *leu9*Δ double mutant and *leu4*Δ *leu9*Δ *leu1*Δ triple mutant unable to synthesize α-IPM, *BAT1* expression was prevented (Figure 6B), further confirmed that *BAT1* Leu3-determined expression is α-IPM dependent. Conversely, *BAT2* expression was very low on glutamine in the wild type, the P_{ENO2}*LEU4* P_{ENO2}*LEU9 leu1*Δ over-expressing, the *leu4*Δ *leu9*Δ and *leu4*Δ *leu9*Δ *leu1*Δ triple mutant strains. In VIL, *BAT2* expression was similarly induced in the α-IPM overproducing strain, and in the null mutant affected in α-IPM

biosynthesis. These results indicate that Leu3-dependent *BAT2* transcriptional regulation does not follow the canonical model proposed for the action of Leu3 as transcriptional modulator (Sze *et al*. 1992), since *BAT2* expression on glutamine or VIL does not respond to α-IPM increased or null levels. These results suggest that for *BAT1*, Leu3-α-IPM abundance directly determines induced expression, while for *BAT2* Leu3-dependent transcriptional modulation could be indirect eliciting the action of a positive regulator whose function is only evident in a *leu3*Δ null mutant. This proposition is supported by the fact that as above presented, although Leu3 can bind both *BAT1* and *BAT2* promoters (Figure 5D), a *leu3*Δ *cis* mutant in the *BAT2* promoter does not mimic the phenotype of a *leu3*Δ mutant and *BAT2* expression is not de-repressed on glutamine (Figure 5F). Furthermore, we performed a qChIP assay using anti-Myc antibody as described in Materials and Methods, on extracts prepared from cultures of the CLA11-735 *LEU3-myc*^{13} *leu3*$_{box}$ strain. As expected, no Leu3-*myc*^{13} immunoprecipitation was observed, confirming the indirect action of Leu3 on *BAT2* expression (Figure 7A).

To analyze Leu3 presumed indirect role on *BAT2* glutamine dependent repression, the *gcn4*Δ *leu3*Δ mutant was constructed as described in Materials and Methods. Northern blot analysis of *BAT2* expression on total RNA samples prepared from cells grown on glutamine as sole nitrogen source, showed that Leu3-dependent *BAT2* de-repression in a *leu3*Δ mutant was not observed in a double mutant *gcn4*Δ *leu3*Δ (Figure 7C). Thus, Leu3 dependent *BAT2* "repression" pattern was the result of the lack of *GCN4* expression whose action is elicited in a *leu3*Δ mutant. Considering that Leu3-α-IPM positively regulates several biosynthetic genes such as *GDH1* (Hu *et al*. 1995), *BAT1*, *LEU1*, *LEU2*, *LEU4* and *ILV5* (Boer *et al*. 2005), in a *leu3*Δ mutant, an amino acid deprivation could be evoked. In

fact, as Table 2 shows, valine, leucine, glutamic acid, alanine and histidine pools are decreased in a *leu3*Δ mutant, during early exponential growth phase (OD_{600} 0.3), on glutamine as sole nitrogen source, as compared with those observed in a wild- type strain. At exponential phase (OD_{600} 0.6), *leu3*Δ amino acid pools recover wild-type concentrations. As shown in Figure 7C, *HIS4* expression is incremented in a *leu3*Δ, but not in a *gcn4*Δ *leu3*Δ. It can be thus concluded that Leu3 dependent *BAT2* expression on glutamine in a *leu3*Δ mutant, is triggered through *GCN4* dependent transcriptional activation, due to Gcn4 increased biosynthesis provoked by amino acid deprivation (Hinnebusch and Fink 1983). To further support this proposition, Gcn4-*myc*^{13} strain was constructed and Gcn4 immunoprecipitation was analyzed in a wild type strain and in a *leu3*Δ mutant (Figure 7B). Gcn4 immunoprecipitation was seven-fold increased in a *leu3*Δ mutant background indicating a higher Gcn4 content. The fact that in both, the *leu4*Δ *leu9*Δ double mutant, and *leu4*Δ *leu9*Δ *leu1*Δ triple mutant (Figure 6A), decreased or null α-IPM biosynthesis did not result in *BAT2* derepression as it occurs in a *leu3*Δ mutant (Figure 5A and Figure 6B), can be explained, since both the double and triple mutants are leucine auxotrophs and have to be grown in the presence of leucine. In all organisms from yeasts to mammals, the target of rapamycin TORC1 pathway controls growth in response to nutrients such as leucine. This amino acid is capable of activating TORC1 kinase, resulting in *GCN4* repression and prevention of TOR-dependent m*GCN4* translation (Kerkhoven *et al*, 2017; Kingsbury *et al*, 2015, Valenzuela *et al*, 2001). This contention is also supported by the herein presented observation that in the presence of VIL Gcn4-*myc*^{13} is poorly immunoprecipitated to the *BAT1* and *HIS4* promoters (Figure 4C), as compared to that

observed on glutamine or GABA, suggesting low Gcn4 concentration when cells are grown on VIL.

Table 2. In a *leu3*Δ mutant grown on glutamine as sole nitrogen source, amino acid deprivation is observed.

Amino acids pool (nmol x 10^8 cells)	OD_{600} 0.3		OD_{600} 0.6	
	WT	***leu3*Δ**	**WT**	***leu3*Δ**
Valine	1,4	0,64	0,71	0,97
Isoleucine	0,62	0,51	0,41	0,57
Leucine	1,07	0,73	0,69	0,72
Glutamic acid	30,63	8,89	16,26	15,25
Alanine	25,08	5,99	13,58	6,39
Histidine	8,21	4,09	4,23	5,74
Asparagine	0,39	0,43	0,25	0,43
Arginine	1,91	2,44	1,37	2,62
Lysine	1,77	4,5	1,22	9
Tryptophan	0,23	0,23	0,19	0,17

The fact that *BAT2* expression was repressed on glutamine and induced on VIL suggested it could be a NCR-regulated gene (Blinder and Magasanik 1995; Coffman *et al*. 1995; Courchesne and Magasanik 1988; Minehart and Magasanik 1991). Considering that genes subjected to NCR control are negatively regulated by Ure2, we analyzed whether this factor played a role in *BAT2* expression. As Figure 7D shows, *BAT2* glutamine-dependent repression was alleviated in an *ure2*Δ mutant. In a double *gln3*Δ *ure2*Δ mutant de-repression was not observed, indicating that Ure2 mediated expression is Gln3 dependent, corresponding to an NCR transcriptional regulation profile (Figure 7D). As control, we measured *DAL5* expression, which is a classical NCR-regulated gene. As expected, *DAL5* glutamine dependent repression was prevented in an *ure2*Δ mutant and hampered in a *gln3*Δ *ure2*Δ double mutant (Figure 7D).

Under catabolic conditions (VIL) Put3 hinders <u>BAT1</u> expression through a negative indirect effect and activates <u>BAT2</u> expression

Above presented results (Figure 5A) indicate that Put3 can act as either a positive (*BAT2*) or negative (*BAT1*) regulatory factor, adding a previously unknown function for Put3 as a transcriptional activator (Brandriss 1987). Put3 regulates genes involved in proline utilization, it is constitutively bound to the *PUT1* and *PUT2* promoters, independently of the nitrogen source (Brandriss 1987). However, it only up-regulates those genes in the presence of proline, or other secondary nitrogen sources, eliciting conformational changes, which influence Put3 activation role (Axelrod *et al*. 1991). In addition, Put3 regulates transcription by undergoing differential phosphorylation as a function of the nitrogen source quality, improving its ability to activate its target genes (Huang and Brandriss 2000). Our results indicate that Put3 negative action on *BAT1* is indirect since it does not bind the *BAT1* promoter (Figure 5C) and a mutant affecting the Put3-binding *cis*-acting elements does not result in *BAT1* de-repression (Figure 5E). It could be thus considered that while Put3 directly activates *BAT2* expression, its role as *BAT1* negative modulator is exerted indirectly. Considering that since Leu3-α-IPM is the main *BAT1* transcriptional activator under biosynthetic conditions and that it could constitute the positive signal activating *BAT1* in a *put3*Δ strain, a *put3*Δ *leu3*Δ double mutant was constructed as described in Materials and Methods. Northern blot analysis of *BAT1* on total RNA samples prepared from cells grown on VIL as sole nitrogen source showed that Put3 dependent *BAT1* de-repression was not observed in the double *put3*Δ *leu3*Δ mutant (Figure 8A). Thus, Put3 dependent *BAT1* "repression" pattern is the result of lack of Leu3-α-IPM, indicating that in

a *put3*Δ single mutant an α-IPM biosynthetic pathway should be operating, in order to allow formation of the Leu3-α-IPM activator. As Figure 8A shows, in a *put3*Δ mutant, *LEU1* and *LEU2* are also de-repressed and as well as for *BAT1*, this de-repression is Leu3-dependent. These data suggest that in a *put3*Δ mutant, in the presence of VIL, leucine could be metabolized to α-IPM through the consecutive action of Bat2-Leu2-Leu1 (Figure 1), enabling Leu3-α-IPM formation and thus recovering Leu3 role as transcriptional activator.

To address the question of the mechanism determining Put3 negative role on VIL, it could be considered that since *LEU1* bears a canonical Put3 binding *cis*-acting element (Figure S6), its expression could be negatively regulated by Put3, thus in a *put3*Δ mutant, *LEU1* expression would be enhanced. It has been shown that the *LEU1* encoded isopropylmalate isomerase can reversibly determine α-IPM biosynthesis (Kohlhaw 2003), this could allow formation of Leu3-α-IPM, influencing *LEU2* activation and promoting leucine-dependent Bat2-Leu2-Leu1 α-IPM biosynthesis. To test this possibility a *put3*Δ *leu1*Δ and a *put3*Δ *bat2*Δ double mutants were constructed as described in Material and Methods. As Figure 8B and C shows, in this double mutants neither *BAT1* nor *LEU2* were de-repressed, indicating that Leu1 and Bat2 activities are required for the functioning of the VIL insensitive α-IPM biosynthetic pathway. Worth of mentioning is the fact that above presented results indicate that on VIL, Put3 can act as either positive (*BAT2*) or negative (*LEU1*) modulator; however, the mechanisms underlying this Put3 dual role remain to be addressed.

In conclusion, when VIL is present as sole nitrogen source, Put3 determines *BAT2* transcriptional activation, while it exerts an indirect negative effect on *BAT1* expression, by preventing Leu3-dependent *BAT1* induced expression.

Taken together, above presented results indicate that *BAT1* and *BAT2* have functionally diverged through sub-functionalization of transcriptional regulation, under biosynthetic and catabolic conditions.

Discussion

Aminotransferases constitute an interesting model to study diversification of paralogous genes carrying out two functions, both of which are needed to warrant metabolite provision, and which cannot be differentially improved to carry out either biosynthesis or catabolism, since aminotransferases constitute biosynthetic and catabolic pathways whose opposed action relies on a single catalytic site (Kohlhaw, 1998; Kohlhaw, 2003). After duplication, *S. cerevisiae* retained *BAT1* and *BAT2* paralogous pair encoding BCATs and functional diversification was achieved through differential expression of the paralogous gene pair (Colon *et al*, 2011).

Results presented in this paper indicate that *BAT1* and *BAT2* retention and regulatory diversification has promoted the acquisition of two independent systems, which respond to the metabolic status of the cell: *BAT1* expression activation through Leu3-α-IPM is indirectly determined by a leucine sensitive and a leucine independent pathway for α-IPM biosynthesis, while *BAT2* expression is determined by the quality of the nitrogen source (Gln3) and amino acid availability (Gcn4) (Figure 9).

This study analyzes the roles of *cis* and *trans*-acting elements generating the *BAT1* biosynthetic and *BAT2* catabolic expression profiles, the influence of chromatin organization on *BAT1* and *BAT2* expression profile, and the impact of the cell metabolic status triggering expression.

Leucine-sensitive and leucine-resistant independent α-IPM biosynthetic pathways determine Leu3 role as activator or repressor and BAT1 biosynthetic expression profile

The role of Leu3 on *BAT1* transcriptional activation depends on the biosynthesis and intracellular concentration of α-IPM, which determines whether Leu3 would function as a repressor (Leu3) or an activator (Leu3-α-IPM) (Chin et al 2008; Wang et al, 1999). To this end, two α-IPM biosynthetic pathways contribute to the building up of an α-IPM pool, in the absence of VIL, Leu4 and Leu9 play the major role while in the presence of VIL, in a *put3*Δ genetic background, the consecutive action of Bat2-Leu2-Leu1 determine α-IPM biosynthesis (Figure 1). When VIL is provided, α-IPM biosynthesis through Leu4-Leu4 or Leu4-Leu9 α-isopropylmalate synthase is precluded, limiting Leu3 activation capacity (López *et al*. 2015; Chin *et al*. 2008; Wang *et al*. 1999). *BAT1* VIL-dependent repression could be regarded as a determinant mechanism regulating leucine biosynthesis. To further enhance *BAT1* Leu3-α-IPM dependent transcriptional activation, chromatin configuration favors the localization of the Leu3 binding *cis*-acting element on the Nucleosome Free Region (NFR) in this promoter.

Results presented in this paper show that in *S. cerevisiae*, an alternative α-IPM biosynthetic pathway can operate through the concerted action of Bat2-Leu2-Leu1 constituting a leucine catabolic pathway, which results in VIL-insensitive, α-IPM biosynthesis (Figure 1). Functioning of this pathway occurs only in a *put3*Δ mutant, in which *LEU1* repression is released, since in this genetic background, the *LEU1*-encoded reversible enzyme can catalyze α-IPM biosynthesis from β-IPM (Figure 1) (Kohlhaw, 1988; Yang *et al*, 2005). Consequently, the formation of the Leu3-α-IPM complex activates

LEU2 and *BAT1* expression. Accordingly, *BAT1, LEU1* and *LEU2* expression is not de-repressed neither in the double *put3*Δ *leu3*Δ mutant (Figure 8A), nor in the *put3*Δ *bat2*Δ double mutants (Figure 8C).

Quality of the nitrogen source and amino acid availability determine <u>BAT2</u> biosynthetic or catabolic expression profile

In the *BAT2* promoter, the *LEU3* binding site is nucleosome occluded when the strain is grown on either VIL or glutamine as nitrogen sources; however, the *GLN3* and *GCN4* binding sites are accessible on VIL, and protected on glutamine (Figure 3B). *BAT2* is regulated through a glutamine-dependent negative regulatory control (NCR), which can be relieved in the presence of secondary nitrogen sources such as VIL, conditions under which, Gln3 is nuclearly located and thus able to activate the expression of genes whose products have a compelling role in the catabolism of secondary nitrogen sources such as VIL (Blinder and Magasanik, 1995; Coffman et al, 1995; Courchesne and Magasanik 1988; Minehart and Magasanik 1991). Additionally, an NCR independent mechanism also contributes to *BAT2* repression under biosynthetic conditions (glutamine as sole nitrogen source). In a *leu3*Δ mutant strain, amino acid deprivation is elicited, resulting in Gcn4 enhanced translation thus inducing *BAT2* expression under biosynthetic conditions (Figure 9). Accordingly, in a *gcn4*Δ *leu3*Δ double mutant neither *BAT2* nor *HIS4* derepression was observed (Figure 7C). Thus, *BAT2* restricted transcriptional activation on primary nitrogen sources, limits Bat2 biosynthetic role. However, the independent action of the Gln3 (catabolic) and Gcn4 (biosynthetic) regulators can activate *BAT2*, indicating that the quality

781 of the nitrogen sources and the intrinsic variation of amino acid availability, trigger *BAT2*
782 expression and Bat2-dependent VIL biosynthesis (Figure 9). Bat1 and Bat2 could
783 redundantly determine VIL biosynthesis, through either Leu3 and/or Gln3/Gcn4
784 transcriptional activation, since in the presence of secondary nitrogen sources, Gln3 and
785 Gcn4 concurrent action would increase *BAT2* expression. Most important is the fact that
786 Bat2 can play a role on either VIL biosynthesis or degradation and the only constraint
787 would be *BAT2* mRNA synthesis and translation.

788 In the presence of a secondary nitrogen source, VIL biosynthesis could be triggered
789 through the concerted action of Bat1 and Bat2, which represents a gene dosage advantage
790 allowing higher biosynthetic capacity. Thus, the acquisition of regulatory systems which
791 allow *BAT1* and *BAT2* expression under biosynthetic and catabolic conditions offers the
792 possibility that Bat1 and Bat2 can play a biosynthetic or catabolic role depending on the
793 reactant intracellular concentration.
794
795
796
797
798
799
800
801
802
803
804

Acknowledgments

We thank Harald Berger and Christoph Schüller for sharing their valuable knowledge, Javier Montalvo-Arredondo, Beatriz Aguirre-López, Juan Carlos Martínez Morales and Eva Klopf for helpful technical assistance, and Rocio Romualdo Martínez for secretarial support.

This study was performed in partial fulfillment of the requirements for the PhD degree in Biochemical Sciences of James Enrique González Flores at the Universidad Nacional Autónoma de México, which he carried with a CONACYT doctoral fellowship. This project was supported by Dirección de Asuntos del Personal Académico Grant/Award Number: IN201015, and by Consejo Nacional de Ciencia y Tecnología, Grant/Award Number: CB-2014-239492-B.

Author contributions: J.G., and A.G. conceived and designed the experiments; J.G., G.L., S.A., M.H., and C.C-B. conducted experiments; J.G., X.E-F., J.S., L.R-R., and A.G. analyzed the data; L.R-R., and J.S. contributed reagents/materials/analysis tools; J.G., and A.G. wrote the manuscript.

Literature Cited

Avendaño, A., L. Riego, A. DeLuna, C. Aranda, G. Romero, C. Ishida *et al.*, 2005 Swi/SNF-GCN5-dependent chromatin remodelling determines induced expression of *GDH3*, one of the paralogous genes responsible for ammonium assimilation and glutamate biosynthesis in *Saccharomyces cerevisiae*. Mol. Microbiol. 57 (1): 291-305.

Axelrod, J. D., J. Majors, M. C. Brandriss, 1991 Proline-independent binding of *PUT3* transcriptional activator protein detected by footprinting in vivo. Mol. Cell. Biol. 11: 564-567.

Biddick, RK, G.L. Law, E. T. Young, 2008 Adr1 and Cat8 mediate coactivator recruitment and chromatin remodeling at glucose-regulated genes. PLoS One. 3.

Blinder, D. and B. Magasanik, 1995 Recognition of nitrogen-responsive upstream activation sequences of *Saccharomyces cerevisiae* by the product of the *GLN3* gene. J Bacteriol. 177: 4190-4193.

Boer, V. M., J. M. Daran, M. J. Almering, J. H. de Winde, J. T. Pronk, 2005 Contribution of the *Saccharomyces cerevisiae* transcriptional regulator Leu3p to physiology and gene expression in nitrogen- and carbon-limited chemostat cultures. FEMS Yeast Res. 5: 885-897.

Brandriss, M. C., 1987 Evidence for positive regulation of the proline utilization pathway in *Saccharomyces cerevisiae*. Genetics. 117:429-35.

Byrne KP and Wolfe KH, 2005 The Yeast Gene Order Browser: combining curated homology and syntenic context reveals gene fate in polyploid species. Genome Res. 15:1456-1461.

Bysani, N., J. R. Daugherty, T. G. Cooper, 1991 Saturation mutagenesis of the UASNTR (GATAA) responsible for nitrogen catabolite repression-sensitive transcriptional activation of the allantoin pathway genes in *Saccharomyces cerevisiae*. J. Bacteriol. 173:4977-82.

Chin, C. S., V. Chubukov, E. R. Jolly, J. DeRisi, H. Li, 2008 Dynamics and design principles of a basic regulatory architecture controlling metabolic pathways. PLoS Biol. 17.

Coffman, J. A., R. Rai, T. G. Cooper, 1995 Genetic evidence for Gln3p-independent, nitrogen catabolite repression-sensitive gene expression in *Saccharomyces cerevisiae*. J. Bacteriol. 177: 6910-6918.

Colón, M., F. Hernández, K. López, H. Quezada, J. González *et al*., 2011 *Saccharomyces cerevisiae* Bat1 and Bat2 Aminotransferases have functionally diverged from the ancestral-like *Kluyveromyces lactis* orthologous enzyme. PLoS One. 6(1).

Conant, G. C., and K. H. Wolfe, 2008 Turning a hobby into a job: how duplicated genes find new functions. Nature Rev. Genet. 9: 938-950.

Courchesne, W. E., and B. Magasanik, 1988 Regulation of nitrogen assimilation in *Saccharomyces cerevisiae*: roles of the *URE2* and *GLN3* genes. J. Bacteriol. 170: 708-713.

De Boer C. G., T. R. Hughes, 2012 YeTFaSCo: a database of evaluated yeast transcription factor sequence specificities. Nucleic Acids Res. 2012 Jan; 40 (Database issue):D169-79.

DeLuna, A., A. Avendano, L. Riego, A. Gonzalez, 2001 NADP-glutamate dehydrogenase isoenzymes of *Saccharomyces cerevisiae*. Purification, kinetic properties, and physiological roles. J. Biol. Chem. 276: 43775-43783.

869 Eden, A, L. Van Nedervelde, M. Drukker, N. Benvenisty, A. Debourg, 2001 Involvement
870 of branched-chain amino acid aminotransferases in the production of fusel alcohols
871 during fermentation in yeast. Appl. Microbiol. Biotechnol. 55: 296-300.
872 Friden, P., and P. Schimmel, 1988 *LEU3* of *Saccharomyces cerevisiae* activates multiple
873 genes for branched-chain amino acid biosynthesis by binding to a common
874 decanucleotide core sequence. Mol. Cell. Biol. 8: 2690-2697.
875 Goldstein, A. L., and J. H. McCusker, 1999 Three new dominant drug resistance cassettes
876 for gene disruption in *Saccharomyces cerevisiae*. Yeast. 15: 1541-1553.
877 Gu, Z., S. A. Rifkin, K. P. White, W. H. Li, 2004 Duplicate genes increase gene expression
878 diversity within and between species. Nat. Genet. 36: 577-579.
879 Gu, X., Z. Zhang, W. Huang, 2005 Rapid evolution of expression and regulatory
880 divergences after yeast gene duplication. Proc. Natl. Acad. Sci. 102: 707-712.
881 Guarente, L., B. Lalonde, P. Gifford, E. Alani, 1984 Distinctly regulated tandem upstream
882 activation sites mediate catabolite repression of the *CYC1* gene of *S. cerevisiae*. Cell.
883 36: 503-11.
884 Hernández, H., C. Aranda, G. López, L. Riego, A. González, 2011 Hap2-3-5-Gln3
885 determine transcriptional activation of *GDH1* and *ASN1* under repressive nitrogen
886 conditions in the yeast *Saccharomyces cerevisiae*. Microbiology. 157: 879-889.
887 Hinnebusch, A. G., and G. R. Fink, 1983 Positive regulation in the general amino acid
888 control of *Saccharomyces cerevisiae*. Proc. Natl. Acad. Sci. 80:5374-8.
889 Hinnebusch, A.G., 1984 Evidence for translational regulation of the activator of general
890 amino acid control in yeast. Proc. Natl. Acad. Sci. 81: 6442-6446.
891 Hinnebusch, A. G., 2005 Translational regulation of *GCN4* and the general amino acid
892 control of yeast. Annu. Rev. Microbiol. 59:407-50.

Hu, Y., T. G. Cooper, G. B. Kohlhaw, 1995 The *Saccharomyces cerevisiae* Leu3 protein activates expression of *GDH1*, a key gene in nitrogen assimilation. Mol. Cell. Biol. 15: 52-57.

Huang, H. L., and M. C. Brandriss, 2000 The regulator of the yeast proline utilization pathway is differentially phosphorylated in response to the quality of the nitrogen source. Mol. Cell. Biol. 20: 892-899.

Infante, J.J., G. L. Law, E. T. Young, 2012 Analysis of nucleosome positioning using a nucleosome-scanning assay. Methods Mol. Biol. 833: 63-87.

Ito, H., Y. Fukuda, K. Murata, A. Kimura, 1983 Transformation of intact yeast cells treated with alkali cations. J. Bacteriol. 153: 163-168.

Kellis, M., B. W. Birren, E. S. Lander, 2004 Proof and evolutionary analysis of ancient genome duplication in the yeast *Saccharomyces cerevisiae*. Nature. 428: 617-624.

Kerkhoven, E. J., Y. Kim, A. Wei, C. D. Nicora, T. L. Fillmore et al, 2017 Leucine biosynthesis is involved in regulating high lipid accumulation in *Yarrowia lipolytica*. mBio. 8: 1-12.

Kingsbury, J. M., N. D. Sen, M. E. Cardenas, 2015 Branched-Chain aminotransferases control TORC1 Signaling in Saccharomyces cerevisiae. PLOS Genetics DOI: 10. 1371/journal.pgen.1005714.

Kispal, G., H. Steiner, D. A. Court, B. Rolinski, R. Lill, 1996 Mitochondrial and cytosolic branched-chain amino acid transaminases from yeast, homologs of the myc oncogene-regulated Eca39 protein. J. Biol. Chem. 271: 24458-24464.

Kohlhaw, G. B., 1988 Isopropylmalate dehydratase from yeast. Methods in Enzymol. 166: 423-429.

916 Kohlhaw, G. B., 2003 Leucine biosynthesis in fungi: entering metabolism through the back
917 door. Microbiol. Mol. Biol. Rev. 67: 1-15.
918 Leach, L. J., Z. Zhang, C. Lu, M. J. Kearsey, Z. Luo, 2007 The role of *cis*-regulatory motifs
919 and genetical control of expression in the divergence of yeast duplicate genes. Mol.
920 Biol. Evol. 24: 2556-2565.
921 Litt, M.D., M. Simpson, M. Gaszner, C. D. Allis, G. Felsenfeld, 2001 Correlation between
922 histone lysine methylation and developmental changes at the chicken beta-globin locus.
923 Science. 293: 2453-2455.
924 Longtine, M.S., A. McKenzie, D. J. Demarini, N. G. Shah, A. Wach *et al.*, 1998 Additional
925 modules for versatile and economical PCR-based gene deletion and modification in
926 *Saccharomyces cerevisiae*. Yeast. 14: 953-961.
927 López, G., H. Quezada, M. Duhne, J. González, M. Lezama *et al.*, 2015 Diversification of
928 Paralogous α-Isopropylmalate Synthases by Modulation of Feedback Control and
929 Hetero-Oligomerization in *Saccharomyces cerevisiae*. Eukaryot. Cell. 14: 564-577.
930 Makova, K.D., and W. H. Li, 2003 Divergence in the spatial pattern of gene expression
931 between human duplicate genes. Genome Res. 13: 1638-1645.
932 Marcet-Houben, M., and T. Gabaldón, 2015 Beyond the Whole-Genome Duplication:
933 Phylogenetic Evidence for an Ancient Interspecies Hybridization in the Baker's Yeast
934 Lineage. PLoS Biol. 13:8.
935 Martinez-Montanes, F., A. Rienzo, D. Poveda-Huertes, A. Pascual-Ahuir, M. Proft, 2013
936 Activator and repressor functions of the Mot3 transcription factor in the osmostress
937 response of *Saccharomyces cerevisiae*. Eukaryot Cell. 12: 636-647.
938 Mewes, H. W., K. Albermann, M. Bahr, D. Frishman, A. Gleisner *et al.*, 1997 Overview of
939 the yeast genome. Nature. 387: 7-65.

940 Minehart, P. L., and B. Magasanik, 1991 Sequence and expression of *GLN3*, a positive
941 nitrogen regulatory gene of *Saccharomyces cerevisiae* encoding a protein with a
942 putative zinc finger DNA-binding domain. Mol. Cell. Biol. 11: 6216-6228.
943 Montalvo-Arredondo, J., Á. Jiménez-Benítez, M. Colón-González, J. González-Flores, M.
944 Flores-Villegas *et al.*, 2015 Functional roles of a predicted branched chain
945 aminotransferase encoded by the *LkBAT1* gene of the yeast *Lachancea kluyveri*. Fungal
946 Genet. Biol. 85: 71-82.
947 Ohno, S., 1970 *Evolution by gene duplication*. Springer-Verlag. New York, USA.
948 Quezada, H., C. Aranda, A. DeLuna, H. Hernández, M. L. Calcagno *et al*., 2008
949 Specialization of the paralogue *LYS21* determines lysine biosynthesis under respiratory
950 metabolism in *Saccharomyces cerevisiae*. Microbiology. 154: 1656-1667.
951 Rawal, Y., H. Qiu, A.G. Hinnebusch, 2014 Accumulation of a threonine biosynthetic
952 intermediate attenuates general amino acid control by accelerating degradation of Gcn4
953 via Pho85 and Cdk. PLoS Genet. 10:7.
954 Siddiqui, A. H., and M. C. Brandriss, 1989 The *Saccharomyces cerevisiae PUT3* activator
955 protein associates with proline-specific upstream activation sequences. Mol. Cell. Biol.
956 9: 4706-4712.
957 Sheff, M. A., and K. S. Thorn, 2004 Optimized cassettes for fluorescent protein tagging in
958 *Saccharomyces cerevisiae*. Yeast. 21: 661-670.
959 Storci, F., and M. A. Resnick, 2003 *Delitto perfetto* targeted mutagenesis in yeast with
960 oligonucleotides. Genet Eng. 25: 189-207.
961 Struhl, K., and R. W. Davis, 1981 Transcription of the *his3* gene region in *Saccharomyces*
962 *cerevisiae*. J. Mol. Biol. 152: 535-552.

963 Sze, J.Y., M. Woontner, J. A. Jaehning, G. B. Kohlhaw, 1992 *In vitro* transcriptional
964 activation by a metabolic intermediate: activation by Leu3 depends on alpha-
965 isopropylmalate. Science. 258: 1143-1145.
966 Thomas-Chollier, M., O. Sand, J. V. Turatsinze, R. Janky, M. Defrance *et al.*, 2008 RSAT:
967 regulatory sequence analysis tools. Nucleic Acids Res., 36:119–127.
968 Thomas-Chollier, M., M. Defrance, A. Medina-Rivera, O. Sand, C. Herrmann *et al.*, 2011
969 RSAT: regulatory sequence analysis tools. Nucleic Acids Res. 39:86–91.
970 Turatsinze, J. V., M. Thomas-Chollier, M. Defrance, J. Van Helden, 2008 Using RSAT to
971 scan genome sequences for transcription factor binding sites and *cis*-regulatory
972 modules. Nat. Protoc., 3:1578–1588.
973 Valenzuela, L., P. Ballario, C. Aranda, P. Filetici, A. González, 1998 Regulation of
974 expression of *GLT1*, the gene encoding glutamate synthase in *Saccharomyces*
975 *cerevisiae*. J. Bacteriol. 180: 3533-3540.
976 Valenzuela, L., C. Aranda, A. González, 2001 TOR modulates GCN4-dependent
977 expression of genes turned on by nitrogen limitation. J. Bacteriol 183-2331-2334.
978 Van Helden, J., 2003 Regulatory sequence analysis tools. Nucleic Acids Res. 31: 3593–
979 3596.
980 Wang, D., F. Zheng, S. Holmberg, G. B. Kohlhaw, 1999 Yeast transcriptional regulator
981 Leu3p. Self-masking, specificity of masking, and evidence for regulation by the
982 intracellular level of Leu3p. J. Biol. Chem. 274: 19017-19024.
983 Wolfe, K. H., and D. C. Shields, 1997 Molecular evidence for an ancient duplication of the
984 entire yeast genome. Nature. 387: 708-713.

985 Yang, C. R., B. E. Shapiro, S. P. Hung, E. D. Mjolsness, G.W. Hatfield, 2005 A
986 mathematical model for the branched chain amino acid biosynthetic pathways of
987 *Escherichia coli* K12. J. Biol. Chem. 280: 11224-11232.
988 Zhang, J., 2003 Evolution by gene duplication: an update. Trends Ecol. Evol. 18: 292-298.
989 Zhang, Z., J. Gu, X. Gu, 2004 How much expression divergence after yeast gene
990 duplication could be explained by regulatory motif evolution? Trends Genet. 20: 403-
991 407.
992 Zhou, H., and F. Winston, 2001 *NRG1* is required for glucose repression of the *SUC2* and
993 *GAL* genes of *Saccharomyces cerevisiae*. BMC Genet. 2:5.
994
995

Figure legends

Figure 1. Diagrammatic representation of the branched chain amino acids biosynthetic pathway of *S. cerevisiae.* The proteins that participate in the pathway are Leu4/Leu9 (α-isopropylmalate synthases, which constitute the leucine sensitive α-IPM biosynthetic pathway), Oac1 (mitochondrial inner membrane transporter), Leu1 (isopropyl malate isomerase), Leu2 (β-IPM dehydrogenase), Bat1 (mitochondrial branched chain aminotransferase), Bat2 (cytoplasmic branched chain aminotransferases), Ilv1 (threonine deaminase), Ilv2 (acetolactate synthase), Ilv5 (acetohydroxiacid reductoisomerase), Ilv3 (dihydroxiacid dehydratase), KIC (α-ketoisocaproate), β-IPM (β-isopropylmalate), α-IPM (α-isopropylmalate), PYR (pyruvate), AL (acetolactate), DHIV (α.β-dehydroxyisovalerate), KIV(α-ketoisovalerate), KB (α-ketobutanoate), AHB (α-keto-2-hydroxybutyrate), DHMV (dihydroxymetylvalerate), KMV (α-ketomethylvalerate), THR (threonine). Dotted lines represent negative allosteric feedback loops. Filled circles represent presumed transporters. The expression of the genes (*LEU4*, *ILV2*, *ILV5*, *LEU1*, *LEU2*, *BAT1* and *GDH1*) proceeded by an arrow are positively regulated by Leu3 (green arrows depict transcriptional activation). The leucine sensitive α-IPM pathway is depicted with a purple arrow, while the arrows pertaining the leucine resistant pathway are shaded in blue.

Figure 2. Northern analysis and Nucleosome Scanning Assay (NuSA) indicate that opposed *BAT1* and *BAT2* transcriptional regulation is partially determined by chromatin organization. (**A**) Northern analysis was carried out on total RNA obtained from *S. cerevisiae* wild type strain (CLA11-700). Yeast cultures were grown on 2% glucose

with either glutamine (Gln, 7mM) or Valine (V, 150 mg/l) + Isoleucine (I, 30 mg/l) + Leucine (L, 100 mg/l) (VIL) as sole nitrogen sources, to an OD_{600} 0.5. Filters were sequentially probed with *BAT1* or *BAT2*-specific PCR products as described in Materials and Methods. A 1500 bp *ACT1* DNA PCR fragment was used as loading control, numbers represent means of *BAT1/BAT2* signals normalized to those of *ACT1*. Standard deviation was calculated and corresponds to +/- 0.12. (**B-C**) For NuSA, mono-nucleosomes were prepared from wild type strain cultures grown on Gln (black line) or VIL (grey line), as described in Materials and Methods. NuSA examined nucleosome occupancy at the *BAT1* and *BAT2* locus, including the 5' ± 600 bp of the intergenic region and the 3' ± 200 bp of the *BAT1* (**B**) and *BAT2* (**C**). MNase treated chromatin and purified DNA samples and mononucleosome-sized (140-160) fragments were prepared as described in Materials and Methods. The resulting material was analyzed with a set of overlapping primer pairs covering the *BAT1* and *BAT2* locus (Tables S5 and S6). Relative *BAT1* and *BAT2* MNase protection was calculated as the ratio of template present in MNase digested DNA over the amount of MNase protection observed for the *VCX1* locus, which was used as control. Data are presented as the average of three independent experiments along with the standard error of the mean (SEM). The diagram of the *BAT1* or *BAT2* promoters was extrapolated from the MNase protection data and depicts nucleosome positioning. Grey ovals indicate firmly positioned nucleosomes, while white ovals with dotted border depict relative occupancy. Black arrows indicate transcription activation. Black boxes correspond to the *LEU3* binding site and $TATA_{BOX}$, NFR- Nucleosome Free Region.

Figure 3. *BAT1* and *BAT2* promoters contain predicted *HAP2, GLN3-GAT1, GCN4, LEU3* and *PUT3* binding sites. In addition to the *HAP2, GLN3-GAT1, GCN4, LEU3* and

PUT3, *BAT1* harbors a *MOT3* binding site (**A**) and *BAT2* an *NRG1* binding sequence (**B**). TF binding sites are indicated as vertical colored coded rectangles, as shown in the lower part of the figure. Ovals indicate fixed positioned nucleosomes for each analyzed promoter under Gln or VIL conditions. Double headed arrow points to either closed (Gln) or open (VIL) chromatin structure in the *BAT2* promoter region. NFR- Nucleosome Free Region.

Figure 4. Role of Gcn4 and Gln3 in *BAT1* or *BAT2* expression. (**A**) Northern analysis was carried out on total RNA obtained from the wild type strain and its isogenic *gcn4*Δ and *gln3*Δ derivatives (Table 1). Strains were grown to OD_{600} 0.5, on MM 2% glucose with either glutamine (Gln, 7mM) or Valine (V, 150 mg/l) + Isoleucine (I, 30 mg/l) + Leucine (L, 100 mg/l) (VIL) as sole nitrogen sources. Filters were sequentially probed with *BAT1* and *BAT2* PCR products described in Materials and Methods. A 1500-bp *ACT1* PCR fragment was used as loading control. Numbers represent means of *BAT1/BAT2* signals normalized to those of *ACT1*, and the resulting ratios in the mutants normalized to those in the WT under derepressing conditions for each gene. Standard deviation was found to be +/- 0.10 - 0.12. (**B**) *BAT1* and *BAT2* promoter regions used to carry out qChIP assays. The three regions which were amplified for each promoter after qChIP assays (R1-R3 for *BAT1* promoter and R1'-R3' for *BAT2* promoter) are depicted. (**C-D**) qChIP assays were performed using anti-Myc antibody (9E 11, Santa Cruz Biotechnology) on wild type strains containing myc^{13} epitope-tagged *GCN4-*myc^{13} and *GLN3-*myc^{13} (Table 1). Strains were grown on MM 2% glucose and either glutamine (black bars, Gln 7mM), γ-aminobutiric acid (white bars, GABA 7mM) or Valine (V, 150 mg/l) + Isoleucine (I, 30 mg/l) + Leucine (L, 100 mg/l) (grey bars, VIL) as sole nitrogen sources, to an OD_{600} 0.5. Gcn4 (**C**) and Gln3

(**D**) binding was analyzed by qChIP, as described in Materials and Methods. IP/Input ratios were normalized with the *GRS1* promoter as negative control (glycyl-tRNA synthase), and *HIS4* and *DAL5* promoters were respectively used as positive controls. Data are presented as the average of three independent experiments along with the standard error of the mean (SEM). (**E**-**F**) Schematic representation of *cis*-acting elements (*GLN3*-*GAT1*) present in *BAT1* and *BAT2* promoters and the sequence mutations which were prepared, as described in Materials and Methods. Northern analysis was carried out on total RNA obtained from each mutant. Meaning of numbers is as that described previously in this figure (see subsection A). Strains were grown on Gln (black line) or adding VIL (white line) as described previously in this figure (see subsection A).

Figure 5. Put3 and Leu3 oppositely regulate *BAT1* and *BAT2* expression. (**A**) Northern analysis was carried out on total RNA obtained from the wild type strain and its isogenic *put3*Δ and *leu3*Δ derivatives (Table 1). Strains were grown to OD_{600} 0.5, on MM 2% glucose with either glutamine (Gln, 7mM) or Valine (V, 150 mg/l) + Isoleucine (I, 30 mg/l) + Leucine (L, 100 mg/l) (VIL) as sole nitrogen sources. Filters were sequentially probed with *BAT1* and *BAT2* PCR products described in Materials and Methods. Numbers meaning has been described in Figure 4A. Standard deviation was found to be +/- 0.10 - 0.12. A 1500-bp *ACT1* PCR fragment was used as loading control. (**B**) *BAT1* and *BAT2* promoter regions used to carry out qChIP assays. The three regions which were amplified for each promoter after qChIP assays (R1-R3 for *BAT1* promoter and R1'-R3' for *BAT2* promoter) are depicted. (**C-D**) qChIP assays were performed using anti-Myc antibody (9E 11, Santa Cruz Biotechnology) on wild type strains containing myc^{13} epitope-tagged *LEU3*-myc^{13} (Table 1). For Put3 qChIP, the *PUT3*-TAP mutant from the *Saccharomyces* yeast collection

was used (Table 1). Strains were grown on MM 2% glucose and either glutamine (black bars, Gln 7mM), γ-aminobutiric acid (white bars, GABA 7mM) or Valine (V, 150 mg/l) + Isoleucine (I, 30 mg/l) + Leucine (L, 100 mg/l) (grey bars, VIL) as sole nitrogen sources, to an OD_{600} 0.5. Put3 (**C**) and Leu3 (**D**) binding was analyzed by qChIP, as described in Materials and Methods. IP/Input ratios were normalized with the *GRS1* promoter as negative control, and *PUT1* and *ILV5* promoters were respectively used as positive controls. Data are presented as the average of three independent experiments along with the standard error of the mean (SEM). (**E-F**) Schematic representation of *cis*-acting elements (*PUT3* or *LEU3*) present in *BAT1* and *BAT2* promoters and the sequence mutations which were prepared, as described in Materials and Methods. Northern analysis was carried out on total RNA obtained from each mutant as described previously. Meaning of numbers is as that described in subsection A. Standard deviation was found to be +/- 0.10 - 0.12. Strains were grown on Gln (black line) or adding VIL (white line) as described previously in this figure (see subsection **A**).

Figure 6. Leu3 determines *BAT2* expression through an α-IPM independent mechanism. (**A**) Diagrammatic representation of the effect of a P_{ENO2}*LEU4* P_{ENO2}*LEU9* *leu1*Δ, a *leu4*Δ *leu9*Δ double mutant and a *leu4*Δ *leu9*Δ *leu1*Δ triple mutant on α-IPM biosynthesis. (**B**) Northern analysis was carried out on total RNA samples obtained from wild type strain and its isogenic derivatives P_{ENO2}*LEU4* P_{ENO2}*9* *leu1*Δ triple mutant, *leu4*Δ *leu9*Δ double mutant and a *leu4*Δ *leu9*Δ *leu1*Δ triple mutant (Table 1). Strains were grown to OD_{600} 0.5, on MM 2% glucose with either glutamine (Gln, 7mM) or Valine (V, 150 mg/l) + Isoleucine (I, 30 mg/l) + Leucine (L, 100 mg/l) (VIL) as sole nitrogen sources. Filters

were sequentially probed with *BAT1* and *BAT2* PCR products described in Materials and Methods. A 1500-bp *ACT1* PCR fragment was used as loading control. Meaning of numbers has been described in Figure 4A. Standard deviation was found to be +/- 0.10-0.12.

Figure 7. *BAT2* expression is indirectly determined by Leu3 and Ure2. (**A**-**B**) qChIP assays were performed using anti-Myc antibody (9E 11, Santa Cruz Biotechnology) on wild-type strains containing *myc*^{13} epitope-tagged *LEU3-myc*^{13}, *LEU3-myc*^{13} P_{BAT2} *leu3cis*Δ (**A**), or *GCN4-myc*^{13} and *GCN4-myc*^{13} *leu3*Δ (**B**) (Table 1). Strains were grown on MM 2% glucose with glutamine (Gln, 7mM) as sole nitrogen sources, to an OD_{600} 0.5. Wild type (black bars) and mutants (grey bars) binding was analyzed by qChIP, as described in Materials and Methods. IP/Input ratios were normalized with the *GRS1* promoter as negative control, and *ILV5* or *HIS4* promoter was respectively used as positive control. Data are presented as the average of three independent experiments along with the standard error of the mean (SEM). (**C**-**D**) Northern analysis was carried out on total RNA samples obtained from wild-type strain and its isogeneic derivatives *leu3*Δ, *gcn4*Δ and *gcn4*Δ *leu3*Δ double mutant (**C**), or *ure2*Δ and *gln3*Δ *ure2*Δ double mutant (**D**) (Table 1). Strains were grown to OD_{600} 0.5, on MM 2% glucose with glutamine (Gln, 7mM) as sole nitrogen sources. Filters were sequentially probed with *BAT2* and *HIS4* or *DAL5* PCR products described in Materials and Methods. A 1500-bp *ACT1* PCR fragment was used as loading control. Meaning of numbers has been described in Figure 4A. Standard deviation was found to be +/- 0.10 - 0.12.

Figure 8. *BAT1* expression is indirectly determined by Put3. (**A**) Northern analysis was carried out on total RNA samples obtained from wild-type strain and its isogeneic derivatives *put3*Δ, *leu3*Δ, *put3*Δ *leu3*Δ, *put3*Δ *leu1*Δ or *put3*Δ *bat2*Δ double mutant (Table 1). Strains were grown to OD_{600} 0.5 on MM 2% glucose with Valine (V, 150 mg/l) + Isoleucine (I, 30 mg/l) + Leucine (L, 100 mg/l) (VIL) as sole nitrogen sources. Filters were sequentially probed with *BAT1*, *LEU1* and *LEU2* PCR products as described in Material and Methods. A 1500-bp *ACT1* DNA PCR fragment was used as loading control. Meaning of numbers as described in Figure 4A. Standard deviation was found to be +/- 0.10 - 0.12.

Figure 9. Schematic representation of *BAT1* and *BAT2* regulatory expression profile depicting *trans*-acting elements acting directly or indirectly on biosynthetic and catabolic conditions. (**A**) Transcriptional factors (TFs) with direct regulation on *BAT1/BAT2* expression in glutamine (Gln) or valine, isoleucine and leucine (VIL) as nitrogen sources. Green arrows on *BAT1* and *BAT2* locus (rectangles) indicate transcriptional activation. (**B**) Different scenarios for the biosynthesis or catabolism of branched chain amino acids (BCAAs) in the wild type and various mutants when grown on biosynthetic (Gln) or catabolic (VIL) conditions. Green arrows facing down indicate target gene activation through TFs action. Horizontal black or grey arrows indicate VIL BIOSYNTHESIS or CATABOLISM. This figure highlights the fact that in a *put3*Δ mutant in the presence of VIL, leucine is preferentially catabolyzed to α-isopropylmalate and not to KIC, through the Bat2-Leu2-Leu1 pathway, while valine and isoleucine are catabolized to KIV or KMV (see Figure 1).

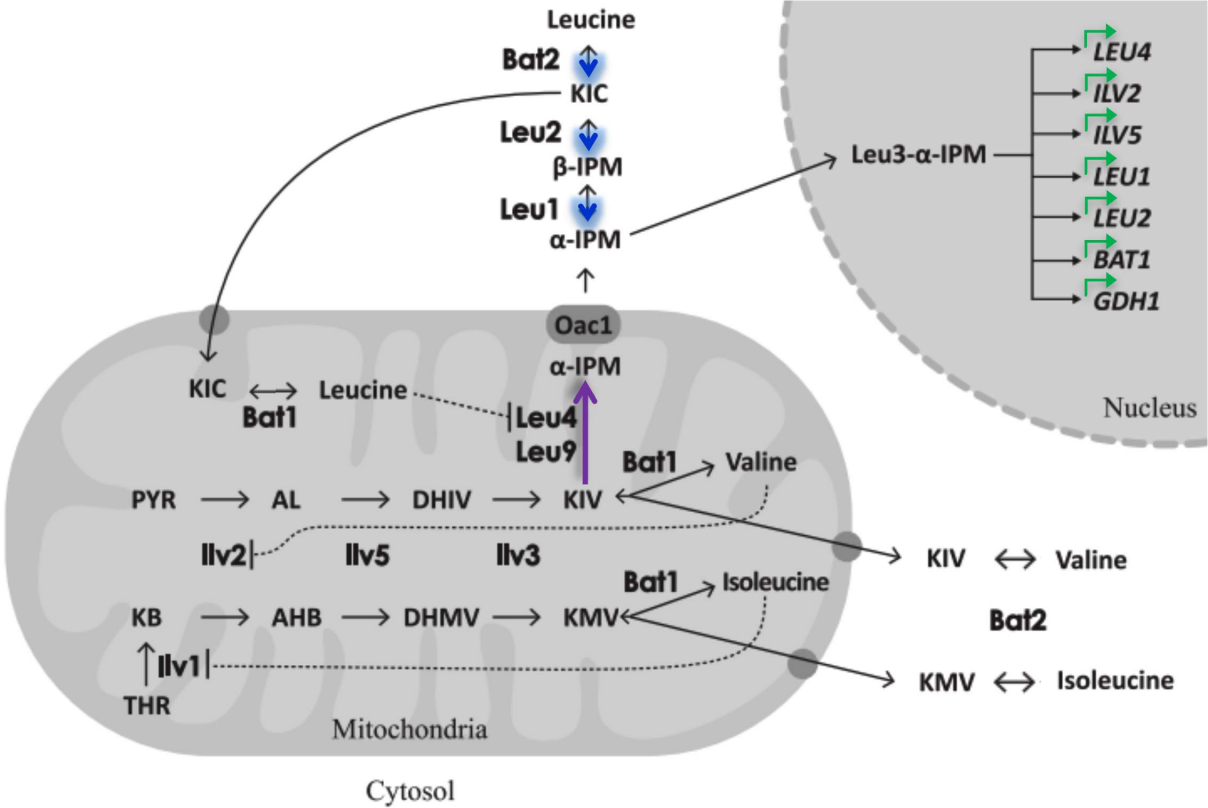
Leucine
Bat2
KIC
Leu2
β-IPM
Leu1
α-IPM
Leu3-α-IPM
LEU4
ILV2
ILV5
LEU1
LEU2
BAT1
GDH1
Nucleus
Oac1
α-IPM
KIC
Bat1
Leucine
Leu4
Leu9
Bat1
Valine
PYR
AL
DHIV
KIV
Ilv2
Ilv5
Ilv3
KIV
Valine
Bat1
Isoleucine
KB
AHB
DHMV
KMV
Bat2
Ilv1
THR
KMV
Isoleucine
Mitochondria
Cytosol

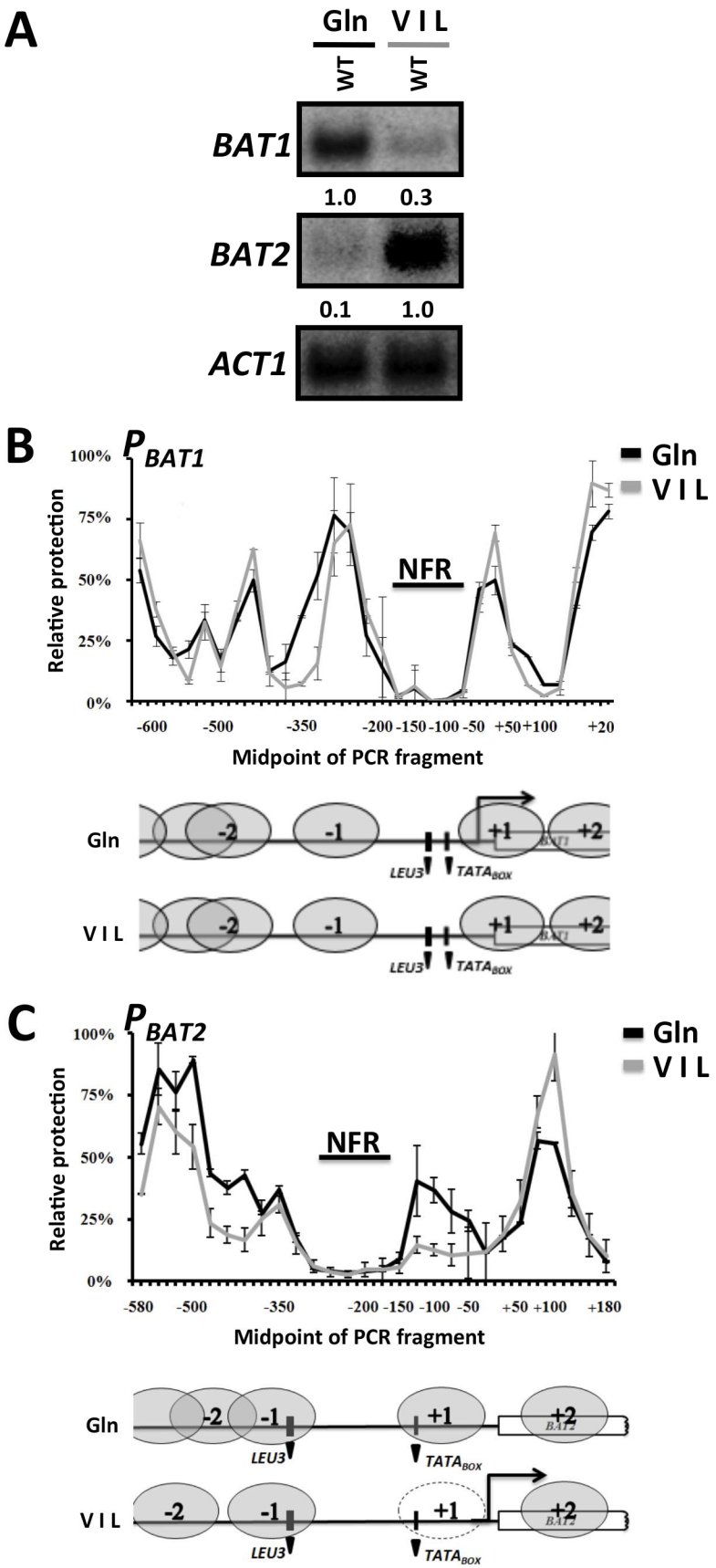
A
Gln
V I L
WT
WT
BAT1
1.0
0.3
BAT2
0.1
1.0
ACT1
B
P BAT1
Gln
V I L
Relative protection
100%
75%
50%
25%
0%
NFR
-600
-500
-350
-200
-150
-100
-50
+50
+100
+20
Midpoint of PCR fragment
Gln
-2
-1
+1
+2
BAT1
LEU3
TATA BOX
V I L
-2
-1
+1
+2
BAT1
LEU3
TATA BOX
C
P BAT2
Gln
V I L
Relative protection
100%
75%
50%
25%
0%
NFR
-580
-500
-350
-200
-150
-100
-50
+50
+100
+180
Midpoint of PCR fragment
Gln
-2
-1
+1
+2
BAT2
LEU3
TATA BOX
V I L
-2
-1
+1
+2
BAT2
LEU3
TATA BOX

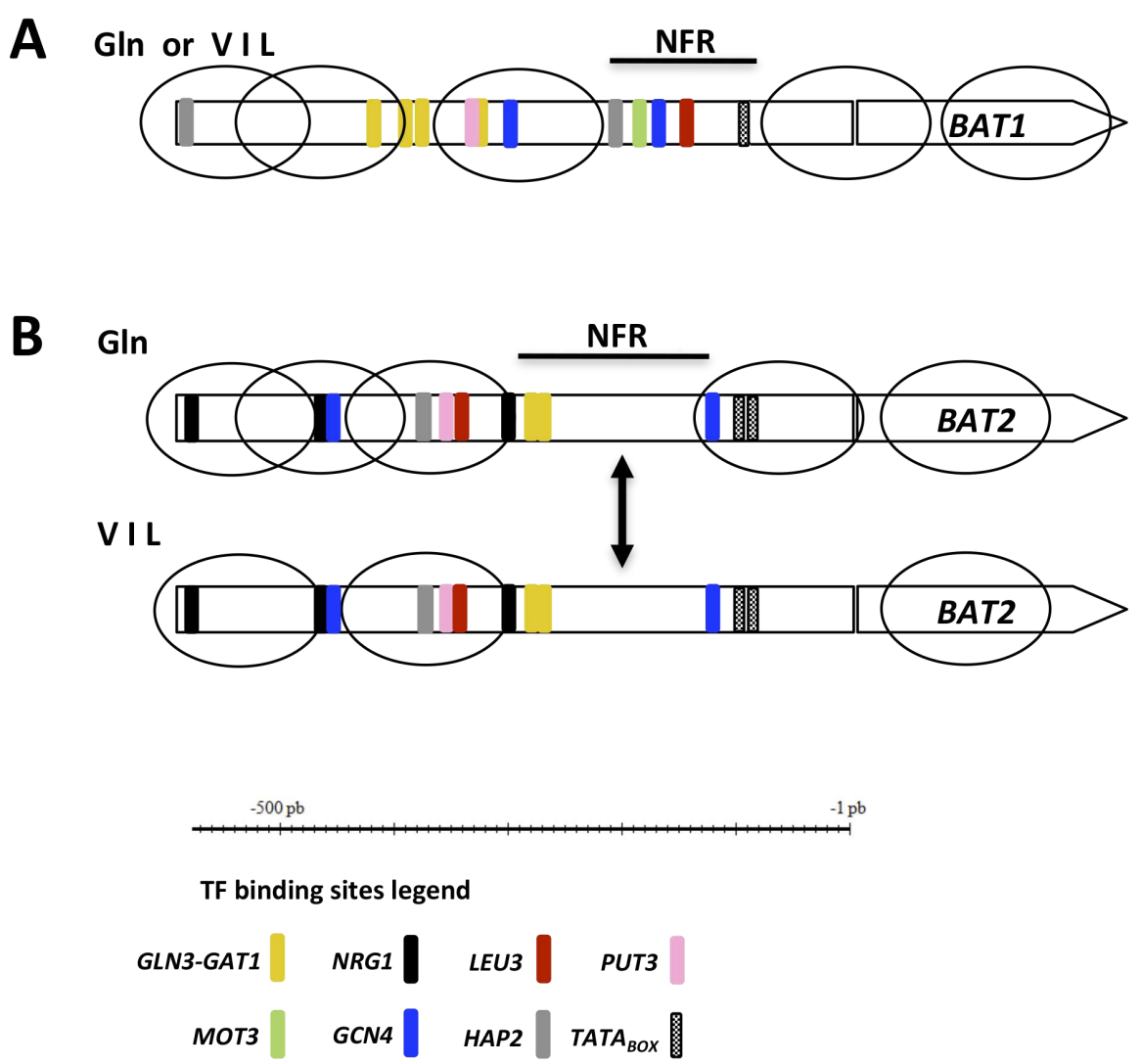
A
Gln or V I L
NFR
BAT1
B
Gln
NFR
BAT2
V I L
BAT2
-500 pb
-1 pb
TF binding sites legend
GLN3-GAT1
NRG1
LEU3
PUT3
MOT3
GCN4
HAP2
TATA BOX

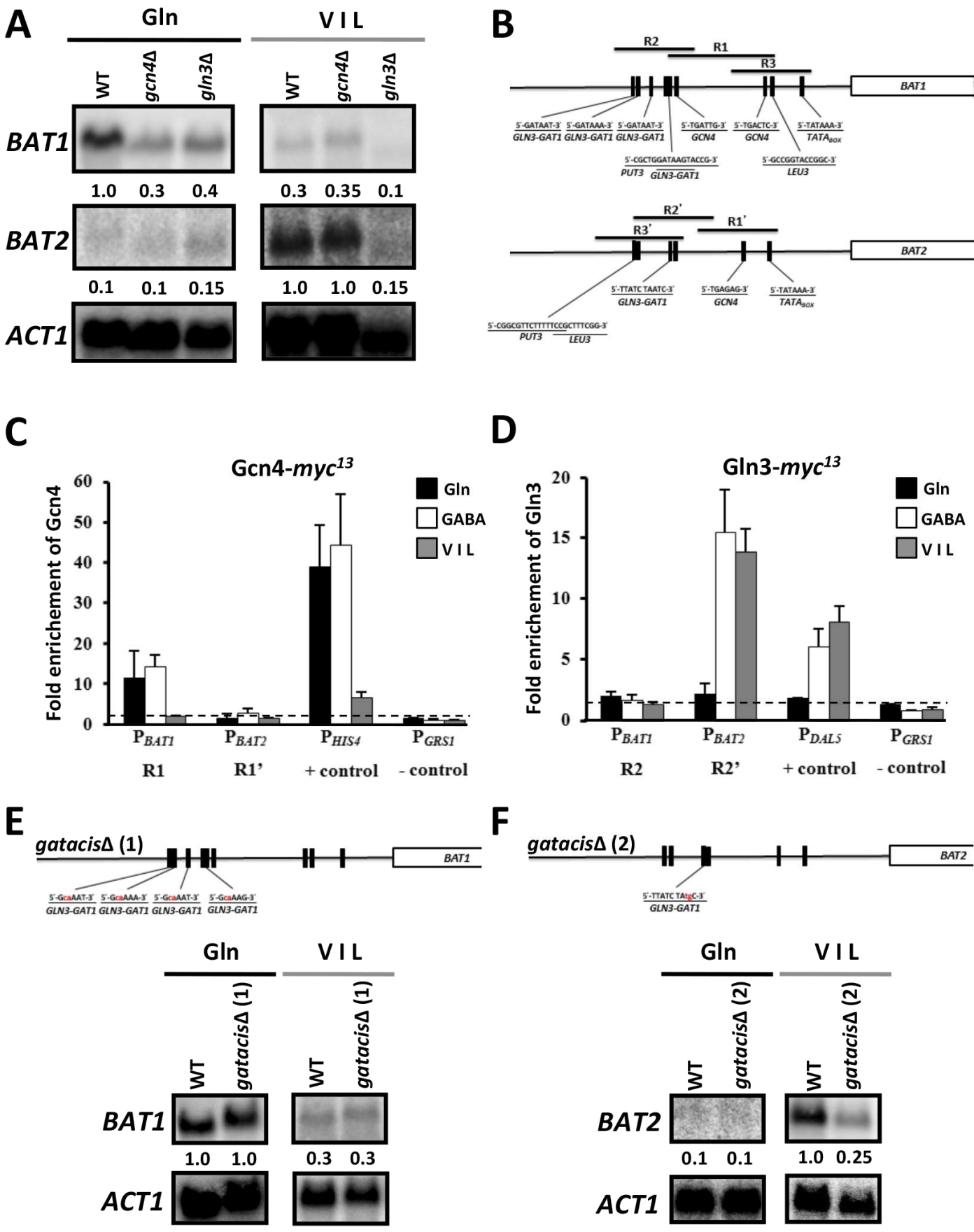
A
Gln
V I L
WT
gcn4Δ
gln3Δ
BAT1
1.0 0.3 0.4
0.3 0.35 0.1
BAT2
0.1 0.1 0.15
1.0 1.0 0.15
ACT1
B
R2
R1
R3
BAT1
5'-GATAAT-3' GLN3-GAT1
5'-GATAAA-3' GLN3-GAT1
5'-GATAAT-3' GLN3-GAT1
5'-TGATTG-3' GCN4
5'-TGACTC-3' GCN4
5'-TATAAA-3' TATA_BOX
5'-CGCTGGATAAGTACCG-3' PUT3 GLN3-GAT1
5'-GCCGGTACCGGC-3' LEU3
R2'
R3'
R1'
BAT2
5'-TTATC TAATC-3' GLN3-GAT1
5'-TGAGAG-3' GCN4
5'-TATAAA-3' TATA_BOX
5'-CGGCGTTCTTTTTCCGCTTTCGG-3' PUT3 LEU3
C
Gcn4-myc13
Fold enrichement of Gcn4
Gln
GABA
V I L
P_BAT1 R1
P_BAT2 R1'
P_HIS4 + control
P_GRS1 - control
D
Gln3-myc13
Fold enrichement of Gln3
Gln
GABA
V I L
P_BAT1 R2
P_BAT2 R2'
P_DAL5 + control
P_GRS1 - control
E
gatacisΔ (1)
BAT1
5'-GcaAAT-3' GLN3-GAT1
5'-GcaAAA-3' GLN3-GAT1
5'-GcaAAT-3' GLN3-GAT1
5'-GcaAAG-3' GLN3-GAT1
Gln
V I L
WT
gatacisΔ (1)
BAT1
1.0 1.0
0.3 0.3
ACT1
F
gatacisΔ (2)
BAT2
5'-TTATC TAtgC-3' GLN3-GAT1
Gln
V I L
WT
gatacisΔ (2)
BAT2
0.1 0.1
1.0 0.25
ACT1

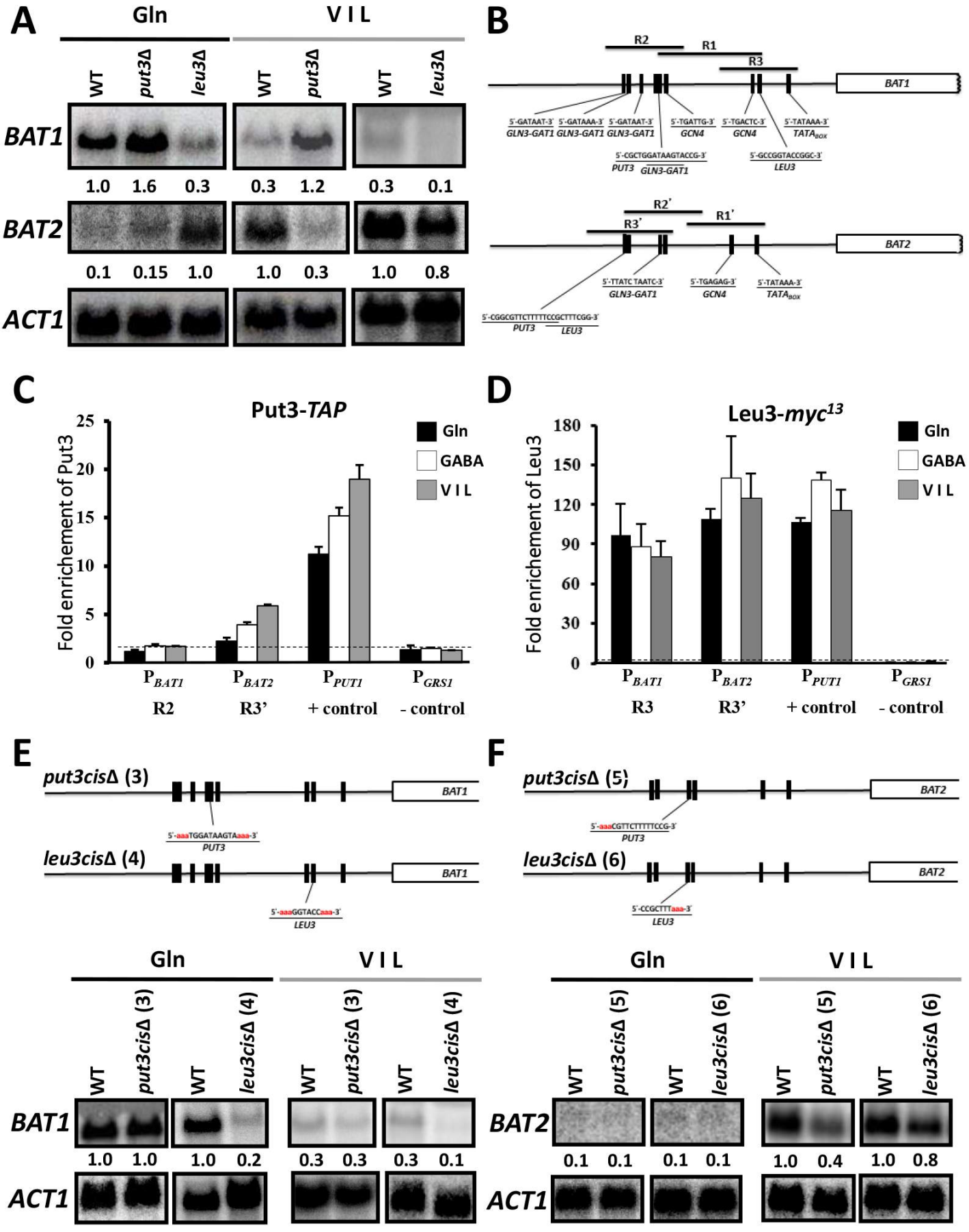
A
Gln
V I L
WT
put3Δ
leu3Δ
WT
put3Δ
WT
leu3Δ
BAT1
1.0 1.6 0.3 0.3 1.2 0.3 0.1
BAT2
0.1 0.15 1.0 1.0 0.3 1.0 0.8
ACT1
B
R2
R1
R3
BAT1
5'-GATAAT-3' GLN3-GAT1
5'-GATAAA-3' GLN3-GAT1
5'-GATAAT-3' GLN3-GAT1
5'-TGATTG-3' GCN4
5'-TGACTC-3' GCN4
5'-TATAAA-3' TATA BOX
5'-CGCTGGATAAGTACCG-3' PUT3 GLN3-GAT1
5'-GCCGGTACCGGC-3' LEU3
R2'
R1'
R3'
BAT2
5'-TTATC TAATC-3' GLN3-GAT1
5'-TGAGAG-3' GCN4
5'-TATAAA-3' TATA BOX
5'-CGGCGTTCTTTTTCCGCTTTCGG-3' PUT3 LEU3
C
Put3-TAP
Fold enrichement of Put3
Gln
GABA
V I L
P BAT1 R2
P BAT2 R3'
P PUT1 + control
P GRS1 - control
D
Leu3-myc13
Fold enrichement of Leu3
Gln
GABA
V I L
P BAT1 R3
P BAT2 R3'
P PUT1 + control
P GRS1 - control
E
put3cisΔ (3)
BAT1
5'-aaaTGGATAAGTAaaa-3' PUT3
leu3cisΔ (4)
BAT1
5'-aaaGGTACCaaa-3' LEU3
F
put3cisΔ (5)
BAT2
5'-aaaCGTTCTTTTTCCG-3' PUT3
leu3cisΔ (6)
BAT2
5'-CCGCTTTaaa-3' LEU3
Gln
V I L
WT
put3cisΔ (3)
WT
leu3cisΔ (4)
WT
WT
BAT1
1.0 1.0 1.0 0.2 0.3 0.3 0.3 0.1
ACT1
Gln
V I L
WT
put3cisΔ (5)
WT
leu3cisΔ (6)
WT
WT
BAT2
0.1 0.1 0.1 0.1 1.0 0.4 1.0 0.8
ACT1

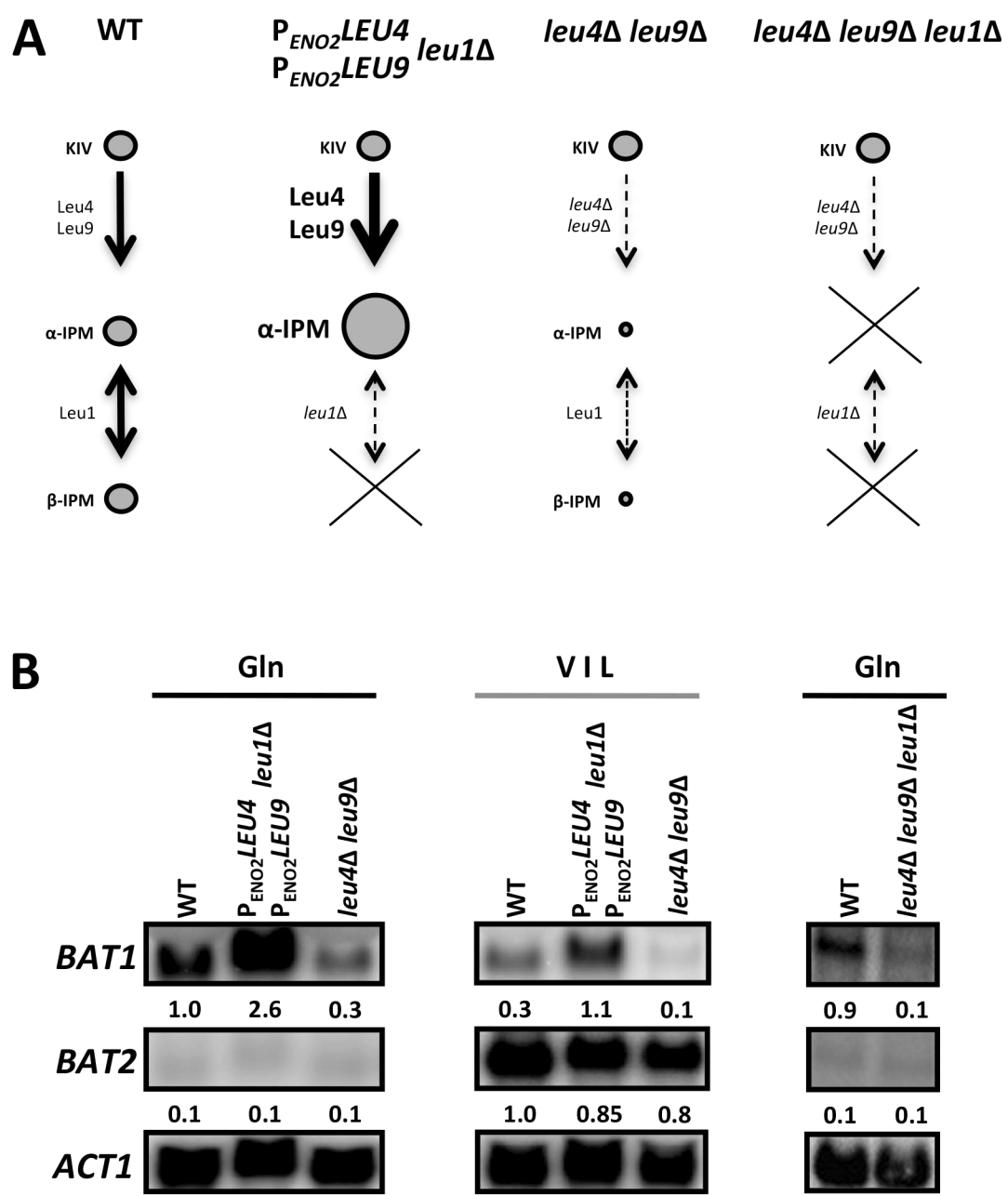
A
WT
P ENO2 LEU4
P ENO2 LEU9 leu1Δ
leu4Δ leu9Δ
leu4Δ leu9Δ leu1Δ
KIV
Leu4
Leu9
α-IPM
Leu1
β-IPM
leu1Δ
leu4Δ
leu9Δ
B
Gln
V I L
Gln
WT
P ENO2 LEU4 leu1Δ
P ENO2 LEU9
leu4Δ leu9Δ
leu4Δ leu9Δ leu1Δ
BAT1
1.0 2.6 0.3
0.3 1.1 0.1
0.9 0.1
BAT2
0.1 0.1 0.1
1.0 0.85 0.8
0.1 0.1
ACT1

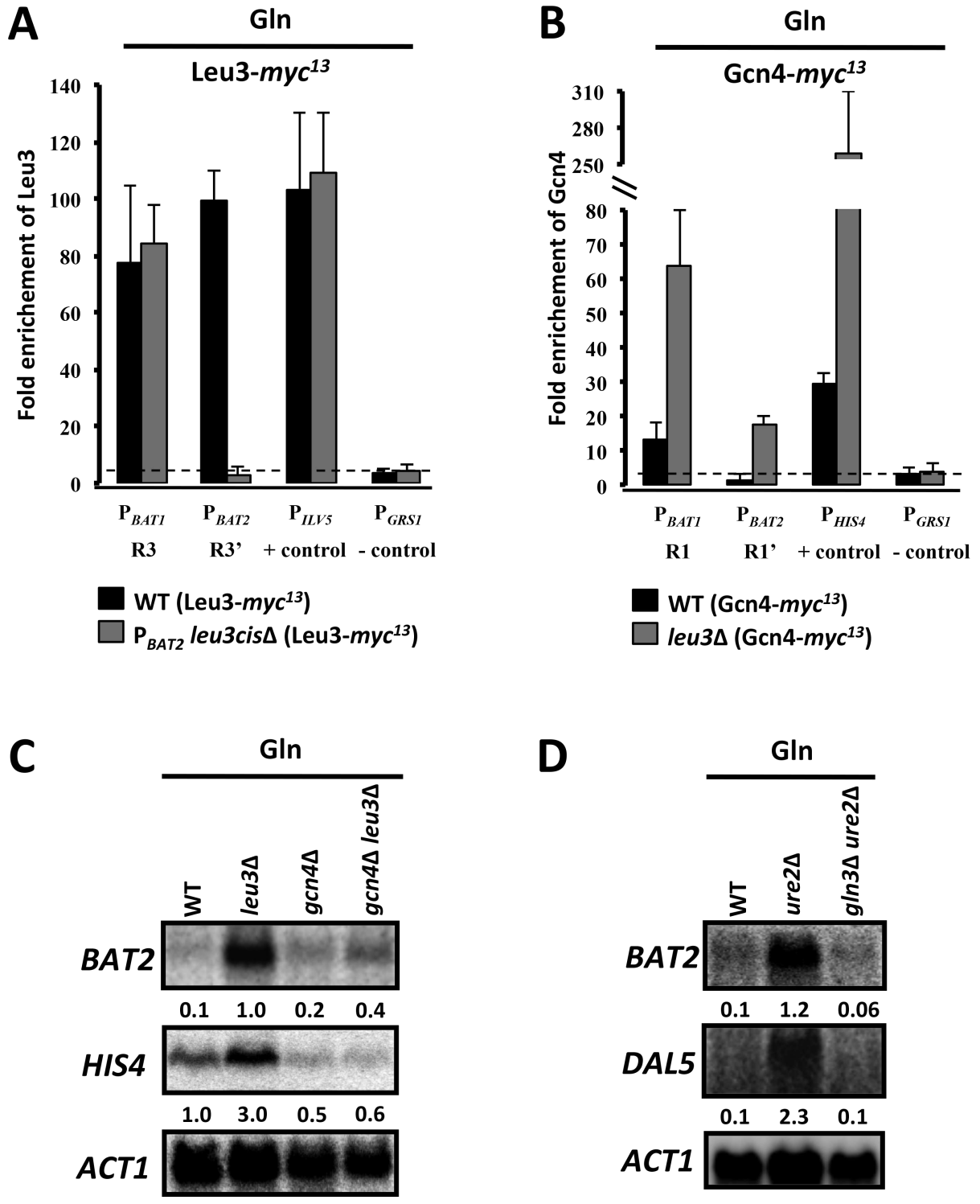
A
Gln
Leu3-myc13
Fold enrichement of Leu3
140
120
100
80
60
40
20
0
P BAT1
P BAT2
P ILV5
P GRS1
R3
R3'
+ control
- control
WT (Leu3-myc13)
P BAT2 leu3cisΔ (Leu3-myc13)
B
Gln
Gcn4-myc13
Fold enrichement of Gcn4
310
280
250
80
70
60
50
40
30
20
10
0
P BAT1
P BAT2
P HIS4
P GRS1
R1
R1'
+ control
- control
WT (Gcn4-myc13)
leu3Δ (Gcn4-myc13)
C
Gln
WT
leu3Δ
gcn4Δ
gcn4Δ leu3Δ
BAT2
0.1
1.0
0.2
0.4
HIS4
1.0
3.0
0.5
0.6
ACT1
D
Gln
WT
ure2Δ
gln3Δ ure2Δ
BAT2
0.1
1.2
0.06
DAL5
0.1
2.3
0.1
ACT1

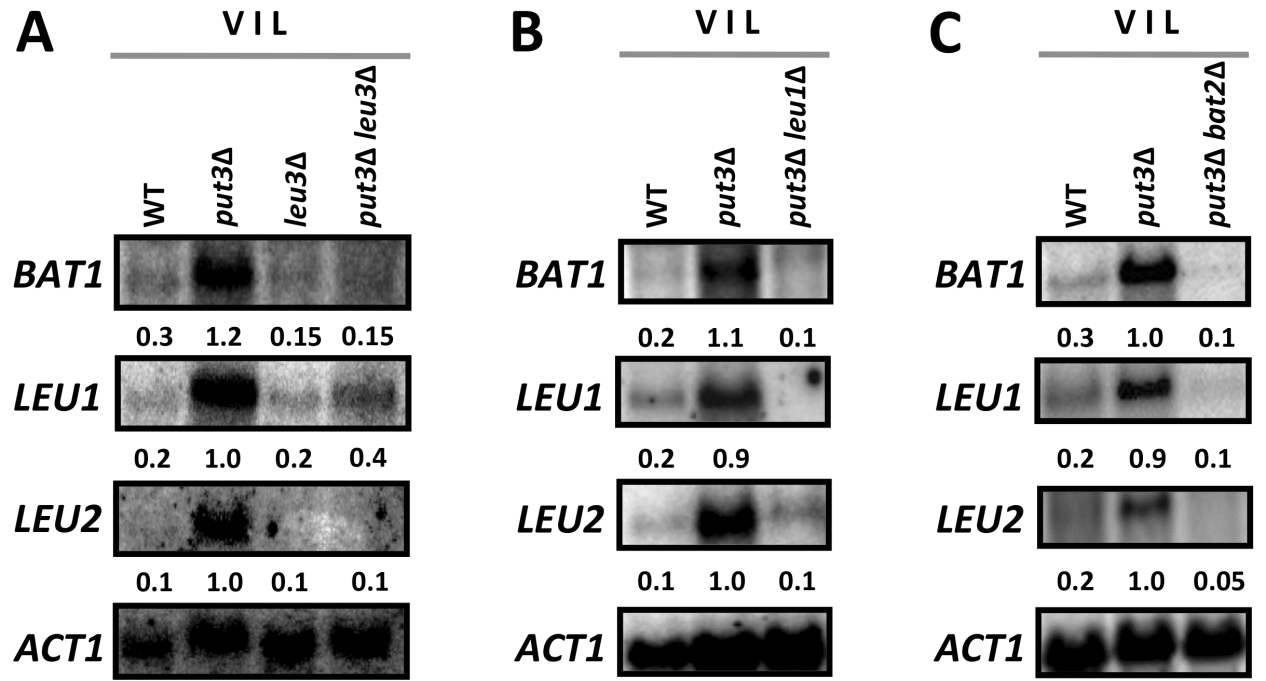
A
VIL
WT
put3Δ
leu3Δ
put3Δ leu3Δ
BAT1
0.3 1.2 0.15 0.15
LEU1
0.2 1.0 0.2 0.4
LEU2
0.1 1.0 0.1 0.1
ACT1
B
VIL
WT
put3Δ
put3Δ leu1Δ
BAT1
0.2 1.1 0.1
LEU1
0.2 0.9
LEU2
0.1 1.0 0.1
ACT1
C
VIL
WT
put3Δ
put3Δ bat2Δ
BAT1
0.3 1.0 0.1
LEU1
0.2 0.9 0.1
LEU2
0.2 1.0 0.05
ACT1

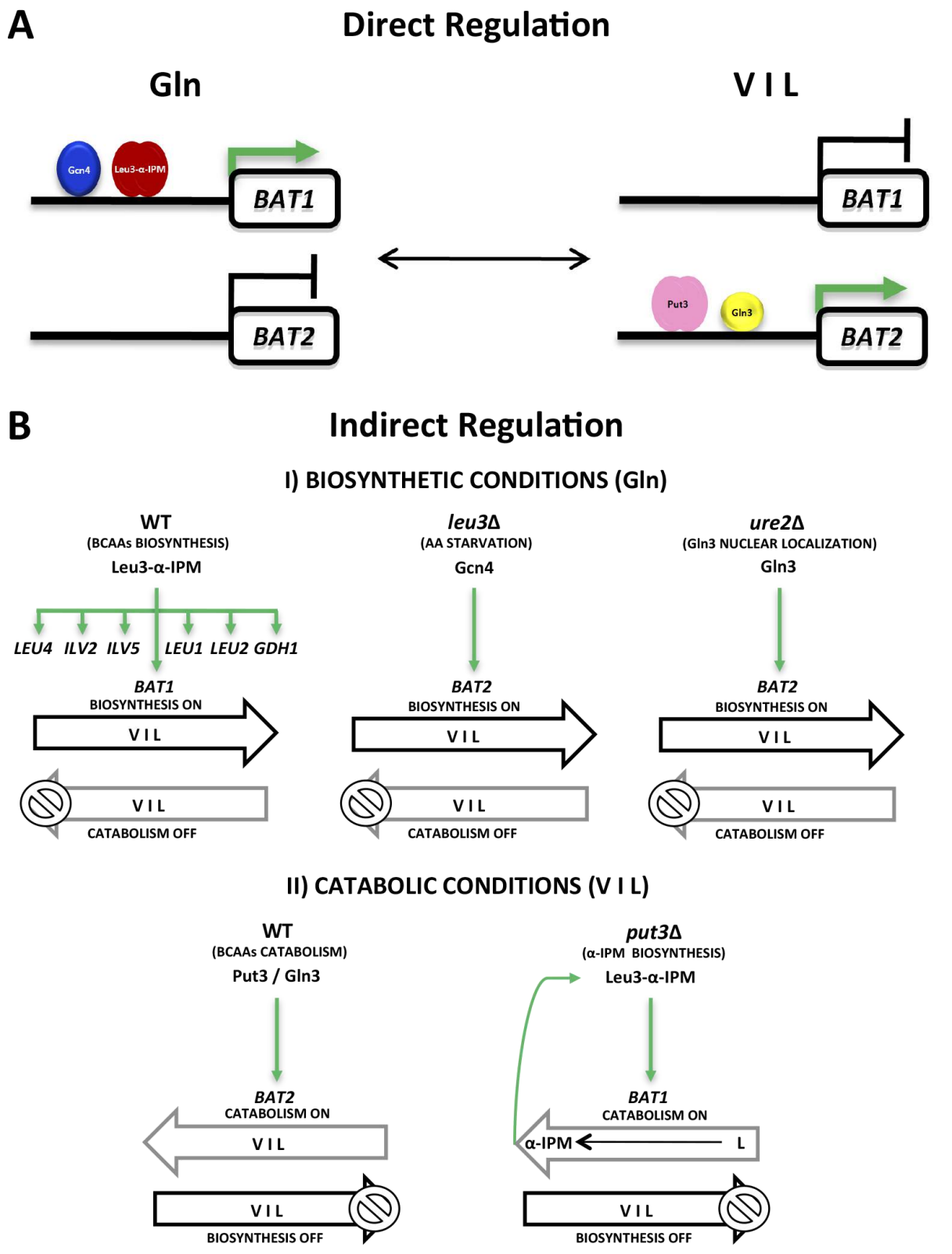
A
Direct Regulation
Gln
V I L
Gcn4
Leu3-α-IPM
BAT1
BAT2
Put3
Gln3
B
Indirect Regulation
I) BIOSYNTHETIC CONDITIONS (Gln)
WT
(BCAAs BIOSYNTHESIS)
Leu3-α-IPM
leu3Δ
(AA STARVATION)
Gcn4
ure2Δ
(Gln3 NUCLEAR LOCALIZATION)
Gln3
LEU4 ILV2 ILV5 LEU1 LEU2 GDH1
BAT1
BIOSYNTHESIS ON
V I L
BAT2
BIOSYNTHESIS ON
V I L
BAT2
BIOSYNTHESIS ON
V I L
V I L
CATABOLISM OFF
V I L
CATABOLISM OFF
V I L
CATABOLISM OFF
II) CATABOLIC CONDITIONS (V I L)
WT
(BCAAs CATABOLISM)
Put3 / Gln3
put3Δ
(α-IPM BIOSYNTHESIS)
Leu3-α-IPM
BAT2
CATABOLISM ON
V I L
BAT1
CATABOLISM ON
α-IPM
L
V I L
BIOSYNTHESIS OFF
V I L
BIOSYNTHESIS OFF